Estimate of changes in agricultural terrestrial nitrogen pathways and ammonia emissions from 1850 to present in the Community Earth System Model

S. N. Riddick[1, 2], D. S. Ward[3,4], P. Hess[1], N. Mahowald[3], R.S. Massad[5] and E.A. Holland[6]

[1] Department of Biological and Environmental Engineering, Cornell University, USA

[2] Centre for Atmospheric Science, Department of Chemistry, University of Cambridge, UK

[3] Department Earth and Atmospheric Sciences, Cornell University, USA

[4] Now at Atmospheric and Oceanic Sciences, Princeton University, Princeton, NJ

[5] INRA, AgroParisTech, UMR1402 ECOSYS, F-78850 Thiverval-Grignon, France

[6] Pacific Centre for Environment and Sustainable Development, University of the South Pacific, Fiji

Corresponding author: Peter Hess, Biological and Environmental Engineering, Cornell University, Ithaca, NY, USA. (peter.hess@cornell.edu)

Abstract. Nitrogen applied to the surface of the land for agricultural purposes represents a significant source of reactive nitrogen (N_r) that can be emitted as a gaseous N_r species, be denitrified to atmospheric nitrogen (N_2), run-off during rain events or form plant useable nitrogen in the soil. To investigate the magnitude, temporal variability and spatial heterogeneity of nitrogen pathways on a global scale from sources of animal manure and synthetic fertilizer, we developed a mechanistic parameterization of these pathways within a global terrestrial model, the Community Land Model (CLM). In this initial version the parameterization emphasizes an explicit climate dependent approach while using highly simplified representations of agricultural practices including manure management and fertilizer application. The climate dependent approach explicitly simulates the relationship between meteorological variables and biogeochemical processes to calculate the volatilization of ammonia (NH_3), nitrification and run-off of N_r following manure or synthetic fertilizer application. For the year 2000, approximately 125 Tg N yr^{-1} and 62 Tg N yr^{-1} is applied to the model land surface as manure and synthetic fertilizer, respectively. We estimate the resulting global NH_3 emissions are 21 Tg N yr^{-1} from manure (17% of manure applied) and 12 Tg N yr^{-1} from fertilizer (19% of fertilizer applied); reactive nitrogen dissolved during rain events is calculated as 11 Tg N yr^{-1} from manure and 5 Tg N yr^{-1} from fertilizer. The remaining nitrogen from manure (93 Tg N yr^{-1}) and synthetic fertilizer (45 Tg N yr^{-1}) is captured by the canopy or transferred to the soil nitrogen pools. In a transient simulation from 1850 to 2000 all nitrogen pathways increase in magnitude as manure and synthetic fertilizer application increase. Partitioning of applied nitrogen in manure to NH_3 emissions increases from 14 % of nitrogen applied (3 Tg NH_3 yr^{-1}) in 1850 to 17% of nitrogen applied in 2000 (21 Tg

NH_3 yr^{-1}). Under current manure and synthetic fertilizer application rates we find a global sensitivity of an additional 1 Tg of NH_3 (approximately 3% of manure and fertilizer) emitted per year ^oC of warming. While the model confirms earlier estimates of nitrogen fluxes made in a range of studies, its key purpose is to provide a theoretical framework that can be employed within a biogeochemical model that can explicitly respond to climate and that can evolve and improve with further observations and characterizations of agricultural practices.

1. Introduction

Nitrogen is needed by all living things for growth. However, it is relatively inert in its most abundant form, diatomic nitrogen (N_2), and needs to be converted to a form of reactive nitrogen (N_r) before it can be used by most plants for growth [Visek, 1984]. Supplying sufficient N_r for maximum crop yield is a major concern in agriculture. In pre-industrial times N_r demand was partly solved with the use of animal manure and seabird guano as well as crop rotation and the use of nitrogen fixing crops [Smil, 2000]. However, by the early 20th century the supply of these N_r sources could not match the demands of an increasing population and a process of creating synthetic N_r was developed: the Haber-Bosch process [Galloway et al., 2004].

The use of N_r to improve crop yield has become an environmental concern as N_r in synthetic fertilizer and manure cascades through the soil, water and the atmospheric nitrogen cycles. Plants can readily use applied N_r for plant growth; however, N_r washed off fields or volatilized as gas can reduce ecosystem biodiversity through acidification and eutrophication [Sutton et al., 2013]. Increased N_r in the hydrosphere can lead to the subsequent degradation of riverine and near shore water quality as the water becomes more acidic and the growth of primary producers blooms [Turner and Rabalais, 1991; Howarth et al., 2002], which can alter the local interspecies competition and biodiversity [Sutton et al., 2012]. Reactive nitrogen emissions into the atmosphere impacts air quality through the ozone generation associated with NO emissions [e.g., Hudman et al., 2010] and the contribution of ammonia (NH_3) to aerosol formation [e.g., Gu et al., 2014]. Nitrogen cycling also impacts climate through the stimulation of plant growth and associated increased carbon storage; through the associated emissions of N_2O, a strong greenhouse gas; through emissions of nitrogen oxides and the associated ozone production; and through the emissions of NH_3 with its potential to cool the climate through aerosol formation [e.g., Adams et al., 2001].

As a result of their dependence on environmental conditions, N_r pathways following manure or synthetic fertilizer application are likely to change in the future under climate change scenarios. This study describes a biogeochemically consistent process driven parameterization suitable for incorporation into Earth System Models that simulates N_r flow following the surface addition of N_r as manure or synthetic fertilizer. The parameterization is evaluated on both the local and global scales against local measurements and global NH_3 flux estimates. The calculated emission estimates for NH_3 and the N_r runoff due to manure and synthetic fertilizer application will be used in ensuing studies in both present and future climates to investigate their impact on nitrogen cycling and climate within the earth system. To our knowledge, no Earth System model has yet to explicitly predict changing nitrogen pathways from manure and synthetic fertilizer in response to climate. We note at the outset that the representation of agricultural processes is highly simplified in the initial model version described here.

Sources of N_r largely fall into two categories, 'new' sources, created by chemical and biological processes, and those that are 'recycled', such as manure excretion of animals. The largest natural new N_r producers are biological nitrogen fixers found in the ocean, biological nitrogen fixers on land, and as the by-product of lightning estimated at 140 Tg N yr^{-1} ± 50%, 58 Tg N yr^{-1} ± 50 % and 5 Tg N yr^{-1} ± 50 %, respectively [Fowler et al., 2013]. The dominant anthropogenic sources of new N_r are Haber-Bosch derived fertilizer (estimated at 120 Tg N yr^{-1} ±10 % in 2005), the burning of fossil fuels, (30 Tg N yr^{-1} ± 10 % in 2000), and a further 60 Tg N yr^{-1} ± 30 % (circa 2005) estimated from biological nitrogen fixers grown for human consumption, such as legumes [Fowler et al., 2013]. Since pre-industrial times, anthropogenic N_r creation has increased from 15 Tg N yr^{-1} to the present estimate of 210 Tg N yr^{-1} [Galloway et al., 2004; Fowler et al., 2013]. Animal manure is used to stimulate plant growth in agriculture. It contains N_r recycled from the soil produced when animals eat plants. A comprehensive increase in livestock population is estimated to have increased global manure production from 21 Tg N yr^{-1} in 1850 to the present estimate of 141 Tg N yr^{-1} [Holland et al., 2005]. It is suggested that this increase in recycled N_r production speeds up the decay and processing of plant biomass, releasing different N_r products to the atmosphere when compared to natural decay processes [Davidson, 2009].

Projections of agricultural activity [Bodirsky et al., 2012] suggest continued increases in the application of synthetic fertilizers until the mid-21st century (and possibly beyond) concurrent with likely increases in manure production [Tilman et al., 2001]. In addition to the increased use of organic and synthetic fertilizers in the future, NH_3 emissions are expected to increase because of the impact of changing climate on nitrogen biogeochemistry [Tilman et al., 2001; Skjoth and Geels, 2013; Sutton et al., 2013].

Current estimates of the direct forcing of nitrate aerosols present as ammonium nitrate encompass the range from -.03 Wm^{-2} to -.41 Wm^{-2} in ACCMIP (Atmospheric Chemistry and Climate Model Intercomparison Project) [Shindell et al., 2013] and AeroCom Phase II [Myhre et. al., 2013] simulations. With a future reduction in sulfate emissions the relative importance of nitrate aerosols is expected to dominate the direct aerosol forcing by 2100 with a resulting increase in radiative forcing of up to a factor of 8.6 over what it would have been otherwise [Hauglustaine et al., 2014]. These estimates do not consider the temperature dependence of NH_3 emissions. Skjoth and Geels [2013] predict increases in future NH_3 emissions of up to 60% over Europe by 2100 largely due to increased NH_3 emissions with temperature. Sutton et al. [2013] predicts future temperature increases may enhance global NH_3 emissions by up to approximately 40% assuming a 5^o C warming. In addition to future changes in climate-induced NH_3 volatilization from manure and synthetic fertilizer application, future changes in agro-management practices, soil microbiological processes and nitrogen runoff may be expected.

Studies calculating NH_3 emission from manure and synthetic fertilizer have broadly fallen into two categories: models that use empirically derived agriculturally-based emission factors and more complex process-based models. Global emissions have almost been universally estimated using the former approach. Emission factors were used by Bouwman et al. [1997] to estimate global NH_3 emissions in 1990 of 54 Tg N yr^{-1}, with the greatest emission of 21.6 Tg N yr^{-1} from domestic animals [Bouwman et al., 1997]. Beusen et al. [2008] also used emission factors to estimate global NH_3 emission from agricultural livestock (21 Tg N yr^{-1}) and synthetic fertilizers (11 Tg N yr^{-1}) in 2000; Bouwman et al. [2013] estimated emissions of 34 Tg NH_3 yr^{-1} on agricultural land, with 10 Tg NH_3 yr^{-1} from animal housing. A number of more recent global models have included emission factors explicitly as a function of temperature [e.g., Huang et al., 2012; Paulot et al., 2014]. Paulot et al. [2014] estimates global current NH_3 emissions of 9.4 Tg yr^{-1} for synthetic fertilizer and 24 Tg yr^{-1} for manure.

Alternatively process-based or mechanistic models have been developed that estimate N_r flows, equilibria and transformations between different nitrogen species as well as nitrogen emissions from synthetic fertilizer and manure. Process models have been used on the field to regional scale, but not on the global scale. These models generally do not simulate the run-off of N_r. For example, Génermont and Cellier [1997] model the transfer of NH_3(g) to the atmosphere after considering the physical and chemical equilibria and transfer of Nr species (NH_3(g), NH_3(aq), NH_4^+(aq)) in the soil. The resulting model is used to calculate the NH_3 emissions from synthetic fertilizer over France within the air quality model, Chimere [Hamaoui-Laguel et al., 2014]. Other examples include Pinder et al. [2004], who describes a process model of NH_3 emissions from a dairy farm, while Li et al. [2013] describes a farm-scale process model of the decomposition and emission of NH_3 from manure.

The overall goal of this paper is to describe and analyze a global model capable of simulating nitrogen pathways from manure and synthetic fertilizer added to the surface of the land under changing climactic conditions to allow a better global quantification of the climate, health and environmental impacts of a changing nitrogen cycle under climate change. The resulting model is of necessity designed for use within an Earth System Model so as to simulate the interactions between the climate and the carbon and nitrogen cycles. Section 2 presents the overall methodology including a detailed description of the process model developed here to calculate climate dependent nitrogen pathways. Section 3 analyzes the model and includes: a comparison of simulated versus site level measurements of NH_3 fluxes; an analysis of the globally heterogeneous nitrogen pathways from applied manure and synthetic fertilizer over a range of climatic regimes; model predictions for changes in nitrogen pathways from 1850 to present and the sensitivity of the results to model parameters. Section 4 gives our conclusions.

2. Methods

In this section we describe a process model for the Flows of Agricultural Nitrogen (FAN) that simulates NH_3 emissions and other N_r flows from applied manure and synthetic fertilizer applications, including their spatial and temporal variations, within an Earth System Model, the Community Earth System Model 1.1 (CESM1.1). The FAN process model developed here simulates the incorporation of manure and fertilizer N_r into soil organic matter and soil nitrogen pools [Chambers et al., 1999], its volatilization as NH_3 to the atmosphere and the direct runoff of N_r from the surface (Figure 1). The model is global in nature, is designed to conserve carbon and nitrogen and responds to changes in climate. It is designed to provide an interface between the application of manure and synthetic fertilizer and the nitrogen cycling developed within the Community Land Model 4.5 (CLM4.5), the land component of the CESM.

Nitrogen pathways subsequent to the application of manure or synthetic fertilizer depend on the complex interaction between both human and natural processes. In particular they depend on the biology and physics of the applied substrate, agricultural practices and climate. Bottom-up emission inventories with specified emission factors that take into account the animal feed, the type of animal housing if any and the field application of the synthetic fertilizer or manure [e.g., Bouwman et al., 1997] are generally used in global chemistry and chemistry-climate applications. For example, this type of emission inventory [e.g. Lamarque et al., 2010] was used in the Atmospheric Chemistry and Climate Model Intercomparison Project (ACCMIP) [Lamarque et al., 2013a] for assessing historical and future chemistry-climate scenarios as well as in assessing nitrogen deposition [Lamarque et al., 2013b] with implications for impacts on the carbon cycle. However, these inventories include very simplified representations of the effect of climate on emissions, for example, by grouping countries into industrial or developing categories [Bouwman et al., 1997]. A seasonal emission dependence is not implicit in these bottom-up inventories although sometimes an empirical relationship is applied [e.g., Adams et al., 2001; also see Skjøth et al., 2011].

In the first application of the model described here we take the opposite tact. We have minimized the description of agricultural practices, and instead emphasize a physically based climate dependent biogeochemistry of manure and synthetic fertilizer decomposition and the resultant nitrogen pathways. The truth of the matter, of course, lies somewhere in between: regional and temporal meteorological differences and changes with climate as well as regional agro-management practices and their possible changes impact NH_3 emissions.

We recognize that in this first application we are simplifying many important agro-management processes including: (1) we assume all synthetic fertilizer is urea and the pH of soil is given. Different applied synthetic fertilizers have a strong impact on the pH of the soil-fertilizer mixture with the overall emission factor very dependent on the pH as well as the day since application [Whitehead and Raistrick, 1990]. Urea is the most commonly used synthetic fertilizer accounting for over 50% of the global nitrogenous synthetic fertilizer usage [Gilbert et al., 2006] and has one of the highest emission factors for commonly used synthetic fertilizers [Bouwman et al., 1997]. Emission factors for other types of fertilizers can be significantly smaller. (2) We do not account for manure management practices. Instead we assume all manure is continuously spread onto fields. In a global study Beusen et al. [2008] considered four primary pathways for manure nitrogen: (1) manure nitrogen lost from the system (14% of the manure nitrogen, range 5-

26%), (2) manure nitrogen excreted in animal houses followed by storage and subsequent spreading onto croplands (35% of manure nitrogen; range 24%-51%), (3) manure nitrogen excreted in animal houses followed by storage and subsequent spreading onto pasture lands (7% of manure nitrogen; range 3%-11%), (4) manure nitrogen excreted by grazing animals onto pastures (44% of manure nitrogen; range 29-59%). Of the 42% of manure nitrogen excreted in housing, 20% (range: 12-28%) is emitted as NH_3 from housing and storage facilities [Beusen et al., 2008]. An additional 15-23% of the remaining manure nitrogen is emitted as NH_3 (range: 11-30%) after it is spread onto crop or pasture land. Of the 44% of manure nitrogen excreted by grading animals on pasture land 11-12% (range 6-17%) is emitted as NH_3. Considering these various pathways the overall emission factor for manure nitrogen is estimated as 19% in Beusen et al. [2008] (compare with 17% in this study). (3) We do not account for specific fertilizer application techniques. For example, the soil incorporation of manure leads to a 50% reduction in NH_3 emissions compared to soil broadcasting (Bowman et al., 2002). We recognize that there are large spreads in all these ranges and that regional practices may alter these numbers, although large errors may be unavoidable due to insufficient characterization of regional agro-management practices.

Even though regional differences in agro-management will result in regional differences in NH_3 emissions, traditional bottom-up NH_3 emission inventories do not account for physically based geographical and meteorological influences, including temperature, turbulence and rainfall. However, these are accounted for in the parameterization described below. As with regional differences in agro-management practices, meteorological impacts may also induce large regional and inter-annual variations in NH_3 emissions. For example, increasing the ground temperature from 290° K to 300°K (at a pH of 7) increases the NH_3 emissions by a factor of 3 (section 2.2).

In the present application we also simplify the representation of NH_3 fluxes to the atmosphere. The aerodynamic resistances used to compute the flux of NH_3 to the atmosphere are calculated with the CLM4.5, but due to the configuration of the CLM are not calculated at the plant function type (PFT) level. In addition, the canopy capture of the NH_3 flux is calculated as a global number and not at the PFT level. The simulation of dynamic NH_3 emissions, as described below, with NH_3 emissions responding to temperature on the model timestep, and thus allowing for a regionally resolved flux of NH_3 dependent on diurnal fluctuations in boundary layer turbulence and boundary layer height is a first step in representing the coupling between terrestrial NH_3 fluxes with the atmosphere. Of course high spatial heterogeneity may preclude an accurate local representation of these exchange processes on the approximately 2 x 2 ° grid cell used here, but even on similar coarse resolutions Zhu et al. [2015] show the implementation of a bidirectional scheme has significant global and pronounced regional impacts (e.g, approximately a 44% decrease in NH_3 emissions over China in April).

A number of additional requirements are necessary to model NH_3 emissions following synthetic fertilizer or manure application within an Earth System Model, specifications that are not necessary in more traditional formulations. (1) The model must be global in nature to characterize global interactions between applied N_r and climate. (2) The model must conserve nitrogen. In particular the nitrogen associated with manure does not add new nitrogen to the system, but merely represents a recycling of available nitrogen. Artificial sources or sinks of nitrogen may have serious repercussions especially when simulating the global nitrogen cycle on the timescale of centuries. (3) The model must be able to simulate the changing impact of climate on the fate of manure and synthetic fertilizer N_r. In particular, NH_3 emissions are sensitive to both temperature and to the water content of the soil. In addition the runoff of N_r is likely to change under climate change scenarios. The process model developed here is capable of simulating the physics of changing nitrogen pathways under a changing climate.

An ideal model would incorporate a globally more explicit representation of agro-management practices, including manure treatment (housing, storage and spreading) and fertilizer application [e.g., see Sutton et al., 2013]. It would also include an explicit representation of the bidirectional exchange of NH_3 between the land and atmosphere including the incorporation of PFT dependent canopy deposition and aerodynamic resistances. While the model developed here captures many of the regional and global features seen in models based on emission factors, here we emphasize the importance of regional differences in meteorology.

2.1 Relation between the FAN process model and the CESM1.1

The parameterization developed here acts as the interface between specified manure and synthetic fertilizer application and the CESM1.1. The CESM1.1 simulates atmospheric, ocean, land and sea ice processes, linked together using a coupler, and includes a land

and ocean carbon cycle [Hurrell et al., 2013; Lindsay et al., 2014]. The CESM participates in the Climate Model Intercomparison Project (CMIP5), and has been extensively evaluated in the literature [see Hurrell et al., 2013]. The land model within the CESM1.1, the CLM 4.5 includes representation of surface energy and water fluxes, hydrology, phenology, and the carbon cycle [Lawrence et al., 2007; Oleson et al., 2008]. The CLM simulations can be forced by meteorology (as done here), or as a part of a coupled-carbon-climate model [Lawrence et al., 2007; Oleson et al., 2008]. The current version of the carbon model is an improved version of the coupled-carbon-climate model used in Keppel-Aleks et al. [2013], Lindsay et al., [2014] and Thornton et al., [2009]. The carbon model includes a nitrogen limitation on land carbon uptake, described in Thornton et al. [2007, 2009]. Further improvements have been made to the below ground carbon cycle, as well as other elements of the land model in order to improve its [e.g. Koven et al., 2013; Lawrence et al., 2012]. The impact of increases in nitrogen deposition (NO_y and NH_x from fossil fuels, fires and agriculture [Lamarque et al., 2010]) have been evaluated [Thornton et al., 2007; Thornton et al., 2009] and extensively compared to observations [e.g. Thomas et al., 2013]. The CLM4 has been extensively tested and evaluated by many studies at the global [Lawrence et al., 2007; Oleson et al., 2008; Randerson et al., 2009] and the site [Stoeckli et al., 2008; Randerson et al., 2009] scale. The CLM4.5 retains the basic properties of CLM4 but with improvements to better simulate: (1) water and momentum fluxes at the Earth's surface; (2) carbon and nitrogen dynamics within soils and (3) precipitation run-off rates [Koven et al., 2013].

As described in Koven et al. [2013], the CLM4.5 simulates the basic flows of N_r within soils following the Century N model [Parton et al., 1996, 2001; Grosso et al., 2000] including the processes of nitrification, denitrification, and emissions of N_r and N_2 and the loss of N_r from leaching and runoff. The CLM4.5 also simulates the transfer of N_r between soils and vegetation, and the loss of N_r from fire. Sources of N_r within the CLM4.5 are from biological nitrogen fixation and from surface deposition. The process model developed here adds an additional source of N_r to the CLM4.5, the addition of synthetic fertilizer. It also adds an additional pathway whereby N_r is recycled: the creation and application of manure (Figure 1).

The relation between nitrogen cycling within the FAN process model developed here and that within the atmospheric, land and river components of the Community Earth System Model (CESM1.1) is given in Figure 1. In this first study the subsequent fate of N_r from synthetic fertilizer or manure application as is incorporated into the soil organic matter or the soil nitrogen pools of the CLM4.5 is not considered here (see Figure 1). As described in more detail below fertilizer and manure is not applied to particular PFTs (e.g., pasture or grassland) within the CLM4.5. This is because soil related properties including soil nitrogen are not specified at the PFT level within the CLM4.5, but instead are specified at the column level that includes many PFTs. In practice we expect that the impact of this contamination across PFTs will be small since the major N-application regions (central US, northern India, eastern China) are not PFT-diverse but contain almost exclusively crop and grass PFTs.

Note that as a first approximation the model described here does not simulate the direct emission loss of species other than NH_3. Atmospheric emission losses of N_2O or N_2 (and potentially NO_X) are simulated in the Community Land Model (CLM) 4.5 [Koven et al., 2013], the land component model of the CESM1.1, 'downstream' from the pathways explicitly considered here. In addition, the fate of N_r emitted into the atmosphere as NH_3 directly from synthetic fertilizer or manure is handled by the atmospheric chemistry component of the CESM (CAM-chem) and is not considered here (Figure 1). The run-off of N_r from manure or synthetic fertilizer nitrogen pools has been coupled to the river transport model (RTM) in [Nevison et al., 2016] (Figure 1), but is also not considered here.

2.2 FAN Process Model

A schematic of the overall model analyzed here is given in Figure 1. All the equations and variables used in the model have been collated and are presented in the appendix. The assumptions used in constructing this model are detailed below where appropriate. Sensitivity to model parameters is given in section 3.4. The nitrogen loss pathways are calculated separately for manure and synthetic fertilizer. While this model assumes that synthetic fertilizer application and manure application can take place in the same approximately 2 x 2 ° grid cell, we also assume that manure and synthetic fertilizer are not applied in the exactly the same place. Therefore the NH_3 emissions, the nitrogen incorporation into soil pools, and the nitrogen run-off are separately calculated for manure and synthetic fertilizer in each column. This means that the Total Ammoniacal Nitrogen (TAN) pools (consisting of NH_3(g), NH_3(aq), NH_4^+) for manure and synthetic fertilizer are discrete and hence the nitrogen pathways are not combined.

The application rate and geographical distribution used for manure and synthetic fertilizer application is taken from the synthetic fertilizer application and manure production datasets developed in Potter et al [2010]. These datasets are valid for circa 2000 for synthetic fertilizer and 2007 for manure [Potter et al., 2010]. As discussed above we assume that manure is continuously spread onto fields by-passing the use of animal houses and storage and is spread across all PFTs. Future model versions will refine these initial assumptions.

To adequately model the conversion timescales of N_r input from animals to TAN, it is necessary to separate the manure into different pools depending on the decomposition timescales (sections 2.2.1 and 2.2.2 and Figure 1). A similar strategy was adopted by Li et al. [2013] for manure and is commonly used in simulating litter decomposition. Synthetic fertilizer N_r is added to one pool, where after it decomposes into the TAN pool (Figure 1). Once in the TAN pool N_r (1) washes off during rain events [Brouder et al., 2005]; (2) volatilizes as NH_3 [Sutton et al., 1994; Nemitz et al., 2000] where after it is redeposited onto the canopy (not shown) or enters the atmospherc flow; (3) nitrifies to form nitrate (NO_3^-) [Stange and Neue, 2009]; 4) or is incorporated into the soil nitrogen pools. Nitrate, in turn, becomes incorporated into the soil (Figure 1). A number of other smaller loss processes are not explicitly simulated.

Manure must be added to the model in such a manner as to conserve nitrogen (Figure 1). Here, we assume animals consume carbon and nitrogen from plants and then subsequently excrete this as manure. Within the CLM, carbon and nitrogen in the plant-leaf pool is thus converted to carbon and nitrogen in manure and urine, conserving overall carbon and nitrogen. The conversion rate from carbon and nitrogen in plants to that in manure and urine is set to equal the rate of manure and urine production. The external dataset of Potter [2010] gives the rate of N_r production from animals, and thus allows us to specify the nitrogen flows. The specified C to N ratio in the plant-leaf pool determines the associated carbon flows due to ruminant consumption of plant material. The input manure and urine production rate from animals implicitly includes that produced from transported feed. Thus the subsequent NH_3 emission rate includes the nitrogen contained in transported feed grown elsewhere. Here we make the simplification that the consumption rate of plant matter to balance the manure and urine production is local. That is, we do not explicitly consider the import of animal feed to match the carbon and nitrogen flows associated with manure and urine production. While this is not entirely consistent, the development of the requisite dataset for feedstock flows from 1850-2000 is outside the scope of this study, although such a dataset could be developed in the future. We do not know of an Earth System Model that does consider the anthropogenic import of nitrogen or carbon. This inconsistency could produce cases where there is insufficient local plant material to balance the overall manure and urine production, but this is generally not the case. The parameterization also ignores export of N_r in ruminant products such as milk and protein, which could create an additional source of uncertainty.

2.2.1 Manure and Urine. Prescribed manure (including urine) is input at a constant annual rate ($\alpha_{applied}(m)$) (g m^{-2} s^{-1}) depending on latitude and longitude into the manure nitrogen pools. It is assumed that a fraction (f_u = 0.5) of nitrogen excreted is urine (urea), with the remaining 50 % excreted as faecal matter [Gusman and Marino, 1999]. The excreted urine is directly added to the TAN pool (g N m^{-2}). Faeces are composed of matter with varying carbon to nitrogen ratios that take different times to decompose depending on how easily they can be digested by microbes**.** Excreted faeces are assumed to form three different pools **(**g m^{-2}) depending on their rate of mineralization [e.g., Gusman and Marino, 1999]**:** (1) we assume a fraction f_{un} =5 % is excreted as unavailable nitrogen ($N_{unavailable}$), the lignin component of manure where the nitrogen remains immobilized by bacteria (C:N ratio > 25:1), (2) a fraction f_r =45% goes to the resistant pool ($N_{resistant}$) which forms the cellulose component of manure (C:N ratio *c.* 15:1) which forms TAN relatively slowly; (3) and a fraction f_a =50% goes to the available pool ($N_{available}$) that is readily available to form TAN ($N_{available}$). In reality the fractions within each of these broadly defined pools will be dependent on the type of animal and the type of feed.

The equations governing the three manure pools (see Figure 1) are:

$$dN_{available}/dt = f_a \, x \, \alpha_{applied}(m) - K_a \cdot N_{available} - k_m \cdot N_{available} \quad (1)$$

$$dN_{resistant}/dt = f_r \, x \, \alpha_{applied}(m) - K_r \cdot N_{resistant} - k_m \cdot N_{resistant} \quad (2)$$

$$dN_{unavailable}/dt = f_{un} \, x \, \alpha_{applied}(m) - k_m \cdot N_{unavailable} \quad (3)$$

where $\alpha_{applied}(m)$ is the amount of manure applied (g m^{-2} s^{-1}); f_a, f_r and f_{un} are the fractions of manure applied to each pool; K_a and K_r (s^{-1}) are temperature dependent mineralization rates and k_m (s^{-1}) is the mechanical loss rate of nitrogen out of these manure pools and into soil nitrogen pools. The decay constants, K_a and K_r are measured as the fast and slow decomposition rates for biosolids added to various soils and incubated at 25^o C [Gilmour et al., 2003], where a two-component decay model accurately fit approximately 73% of the samples incubated. The decay timescales for manure are 48 days and 667 days at 25 °C. The temperature dependence of the decay constants is derived from a fit of temperature dependent mineralization rates (see appendix) [Vigil and Kissel, 1995] corresponding to a Q10 value of 3.66. To prevent the manure pools from building up over long-timescales we assume that manure is incorporated into soils with a time constant of 365 days with a mechanical rate constant k_m. This timescale is consistent with the base bioturbation rate of 1 cm^2 year^{-1} assumed in Koven et al. [2013] and a typical length scale of 1 cm. The sensitivity of the subsequent nitrogen pathways to this timescale is small (section 3.4). Note, that nitrogen in the $N_{unavailable}$ pool does not mineralize and is thus only incorporated into soil organic matter on the timescale determined by k_m. We assume nitrogen prior to conversion to TAN comprises a range of insoluble organic compounds that do not wash away or otherwise volatilize.

2.2.2 Synthetic fertilizer. Synthetic fertilizer nitrogen is added to the $N_{fertilizer}$ pool (g N m^{-2}) (Figure 1) at a rate ($\alpha_{applied}(t)(f)$) (g N m^{-2} s^{-1}) that depends on geography and time. The amount of nitrogen within the synthetic fertilizer pool is subsequently released into the TAN pool with the rate k_f (s^{-1}):

$$dN_{fertilizer}/dt = \alpha_{applied}(f) - k_f \cdot N_{fertilizer} \qquad (4)$$

Here we assume all synthetic fertilizer is urea. Urea is the most commonly used synthetic fertilizer accounting for over 50% of the global nitrogenous synthetic fertilizer usage [Gilbert et al., 2006]. Many other fertilizer types have significantly lower emission factors depending largely on changes in soil pH due to interactions between the soil and the fertilizer (Whitehead and Raistrick, 1990). We do not simulate this interaction here, but it should be accounted for in future model development. Thus the estimates here for fertilizer NH_3 emissions may be considered as an upper estimate. We set the decay timescale of urea fertilizer to be 2.4 days consistent with the decay rate measured in Agehara and Warncke [2005] for temperatures from 15 to 20 ^{o}C. In a series of experiments Agehara and Warncke [2005] show that 75% of the urea hydrolyzes in a week at temperatures from 10 to 25 ^{o}C without a significant dependence on temperature especially for temperatures above 15 to 20 ^{o}C.

The timing for synthetic fertilizer application is determined internally within the CLM4.5 crop model as the spring planting date for corn. We use corn since the CLM4.5 crop model only specifically includes corn, soybean and temperate cereals and the planting date for corn lies between the earlier planting date for temperate cereal crops and the later planting of soy. The date for fertilizer application is determined for each grid point location using the surface temperature-based criteria developed by Levis et al. [2012] for simulating the planting date of corn: the ten-day running mean temperature, ten-day running mean daily minimum temperature and growing degree days must all surpass fixed threshold values (283.15K, 279.15K and 50 days, respectively) before planting can take place. We do not use the Levis et al. [2012] crop model in this study but use these criteria to determine a planting date for each grid point and assume synthetic fertilizer is applied on this date. Fertilizer application dates can have a large influence on the seasonality of the emissions (e.g., see Paulot et al., 2014) and the nitrogen loss pathways following fertilization (section 3.4). Future applications will assume more complete algorithms for fertilizing the spectrum of crops, as well as multiple fertilizer applications and double cropping. A global accounting of fertilization practices and application techniques (e.g., fertilizer injection) nevertheless remains a considerable source of uncertainty in global modeling of the NH_3 emissions from agriculture.

2.2.3 Total Ammonical Nitrogen (TAN). We consider two TAN pools (g N m^{-2}), one for the nitrogen produced from synthetic fertilizer $N_{TAN}(f)$ the other for nitrogen from manure $N_{TAN}(m)$. The budget for the manure and synthetic fertilizer TAN pools respectively is given by:

$$N_{TAN}\,(m)/dt = f_u x\ \alpha_{applied}(\mathrm{m}) + K_r \cdot N_{resistant} + K_a \cdot N_{available}$$
$$-F_{run}(m) - K_D^{NH4} \cdot N_{TAN}(m) - F_{NH3}(m) - F_{NO3}(m) \quad (5)$$

$$N_{TAN}\,(f)/dt = k_f \cdot N_{\boldsymbol{fertilizer}}$$
$$-F_{run}(f)\ \ - K_D^{NH4} \cdot N_{TAN}(f) - F_{NH3}(f) - F_{NO3}(f) \quad (6)$$

Here $F_{run}(m/f)$ (g N m^{-2} s^{-1}) is the loss of nitrogen by runoff from the manure or synthetic fertilizer pool, K_D^{NH4} (s^{-1}) the loss rate of nitrogen to the soil nitrogen pools, $F_{NH3}(m)$ *and* $F_{NH3}(f)$ (g N m^{-2} s^{-1}) the NH_3 emissions from the TAN pool to the atmosphere from the soil manure and synthetic fertilizer pools, respectively, and $F_{NO3}(m)$

and $F_{NO3}(f)$ (g N m^{-2} s^{-1}) the loss of nitrogen through nitrification from the manure and synthetic fertilizer pools respectively. The formulation of each of these terms is given below. Inputs into N_{TAN} (m) pool are from the fraction (f_u) of applied manure as urine ($\alpha_{applied}$(m)), and from the decomposition of the nitrogen within the available and resistant manure pools. Input into the N_{TAN} (f) pool is through decomposition of nitrogen within the synthetic fertilizer pool.

2.2.4 Runoff of nitrogen to rivers. The immediate runoff of fertilizer and manure nitrogen to rivers is derived from the runoff rate of water (R) (m s^{-1}) in the CLM multiplied by concentration of nitrogen in the TAN water pool:

$$F_{run}(m/f) = R \cdot \frac{N_{TAN}(m/f)}{N_{water}(m/f)}. \quad (7)$$

The value of R is calculated within the CLM and is a function of precipitation, evaporation, drainage and soil saturation. The amount of water within the TAN pool ($N_{water}(m/f)$)(m) is needed to convert N_{TAN} (g N m^{-2}) to a concentration (g N m^{-3}). An expression for $N_{water}(m/f)$ is given in Section 2.2.9. It should be emphasized that this is the immediate runoff of manure and synthetic fertilizer nitrogen from the TAN pools. Subsequent loss of nitrogen derived from manure and synthetic fertilizer application occurs following the nitrogen transfer to the soil pools, but is not tracked in these simulations. Additional hydrological losses will also occur following NH_3 volatilization to the atmosphere, the subsequent deposition and loss through runoff or leaching. These losses are also not tracked in the current simulation.

Initially, we attempted to use the runoff parameterization based on the global Nutrient Export from Watersheds 2 (NEWS 2) Model [Mayorga et al., 2010] where runoff is also parameterized in terms of *R*. However, the amount of nitrogen that runs off in NEWS 2 is represented in terms of the annual nitrogen initially applied to the land and thus is not directly related to the amount of nitrogen in the TAN pool.

2.2.5 Diffusion through soil. Nitrogen is assumed to diffuse from the TAN pool to the soil pools. Génermont and Cellier [1997] represent the diffusion coefficient of ammonium through soils as dependent on soil water content, soil porosity, temperature and an empirical diffusion coefficient of ammonium in free water (see appendix). For example, assuming a temperature of 21^{o} C, a soil porosity of 0.5 and a soil water content of 0.2 the resulting diffusion coefficient is approximately 0.03 cm^2 day^{-1}, in reasonable agreement with measurements in Canter et al. [1997]. Here we assume a typical length scale of 1.0 cm to convert the diffusion rate to a timescale. The resulting diffusion of ammonical nitrogen is added to pre-existing nitrogen pools in the CLM4.5 and is not further tracked.

2.2.6 Flux of Ammonia to the Atmosphere. The flux of NH_3 (F_{NH3}, g m^{-2} s^{-1}) to the atmosphere is calculated from the difference between the NH_3 concentration at the surface ($NH_3(g)$, g m^{-3}) of the TAN pool and the free atmosphere NH_3 concentration (χ_a, g m^{-3}) divided by the aerodynamic (R_a) and boundary layer (R_b) resistances (Equation 8) [Nemitz et al., 2000; Loubet et al., 2009, Sutton et al., 2013].

$$F_{NH3} = \frac{NH_3(g) - \chi_a}{R_a(z) + R_b} \qquad (8)$$

The calculation of $NH_3(g)$ is given below. For compatibility with the NH_3 emission model we compute average values of R_a and R_b over each CLM soil column, which may contain several PFTs. Continental NH_3 concentrations between 0.1 and 10 µg m^{-3} have been reported by Zbieranowski and Aherne [2012] and Heald et al. [2012]. We specify χ_a to be 0.3 μg m^{-3}, representative of concentrations over low activity agricultural sites [Zbieranowski and Aherne, 2012]. This concentration is intermediate between concentrations at low to moderate pollution sites as diagnosed in GEOS-chem [Warner et al., 2015]. The sensitivity to this parameter is small as NH_3(g) is usually very large (section 3.4). While equation (8) allows for negative emissions $(\mathrm{NH_3(g)} < \chi_\mathrm{a})$ or deposition of atmospheric NH_3 onto the soil we currently disallow negative emissions in the current simulations. In future studies the atmospheric concentration of NH_3 will be calculated interactively by coupling the FAN model to the atmospheric chemistry componenent of the CESM (CAM-chem), thus allowing the dynamics of the NH_3 exchange between the soil, the atmosphere and vegetation to be captured [e.g., Sutton et al., 2013].

A large fraction of the NH_3 emitted to the atmosphere is assumed captured by vegetation. The amount emitted to the atmosphere is given by:

$$F_{NH3_{atm}}(m/f) = (1 - f_{capture}\ ) \times F_{NH3}(m/f) \quad (9)$$

where $f_{capture}$ is set to 0.6, where this accounts for the capture of the emitted NH_3 by plants or even onto the soil surface. Plant recapture of emitted NH_3 is often reported to be as high as 75 % (Harper et al., 2000; Nemitz et al., 2000; Walker et al. 2006; Denmead et al., 2008; Bash et al., 2010). Using seabird nitrogen on different substrates (rock, sand, soil and vegetation) inside a chamber Riddick (2012) found NH_3 recapture to be 0% on rock, 32% on sand, 59% on soil and 73% on vegetation. We set $f_{capture}$ to 0.6 in-line with the findings of Wilson et al. [2004] as a mid-way between the value for soil (when the crops are planted) to when they are fully grown. Bouwman et al. [1997] also used canopy capture to estimate emissions with the captured fraction ranging from 0.8 in tropical rain forests to 0.5 in other forests to 0.2 for all other vegetation types including grasslands and shrubs. Bouwman et al. [1997] omitted canopy capture over arable lands and intensively used grasslands. Overall, the deposition of NH_3 onto the canopy (or even the soil surface) is poorly constrained [e.g., see Erisman and Draaijers, 1995] and often ignored in model simulations. In reality canopy capture is not constant but depends on surface characteristics and boundary layer meteorology. Variations in canopy capture will induce temporal and regional variations in NH_3 emissions. Explicitly including the canopy capture fraction allows us to explicitly differentiate between different biogeochemical pathways in future studies. In the future when the model is fully coupled with the atmospheric NH_3 cycle a compensation point approach would be desirable for calculating the net NH_3 emissions, but we feel it is outside the scope of the present study.

It is assumed that the nitrogen in the TAN pool is in equilibrium between $NH_3(g)$ (g m^{-3}), $NH_3(aq)$ (g N m^{-3}) and $NH_4^+(aq)$ (g N m^{-3}). The equilibrium that governs the speciation of these species is determined by the Henry's Law coefficient (K_H), where K_H is a measure of the solubility of NH_3 in water, and the disassociation constant of NH_4^+ in water (K_{NH4}) (moles l^{-1}) [e.g., Sutton et al., 1994]

$$NH_3(g) + H_2O \overset{K_H}{\leftrightarrow} NH_3(aq) \quad (10)$$

$$NH_4^+(aq) \quad \xleftrightarrow{K_{NH4}} NH_3(aq) + \ H^+ \quad (11)$$

Combining these two expressions $\mathrm{NH_3(g)}$ can be expressed as a function of the total TAN (e.g., Pinder et al. [2004], although note their different units for K_H and K_{NH4})

$$NH_3(g)(m/f) = \frac{N_{TAN}(m/f)/N_{water}(m/f)}{1+K_H+K_H[H^+]/K_{NH4}} \quad (11)$$

where $[H^+]$ is the hydrogen ion concentration in moles/liter. Both K_H and K_{NH4} are temperature dependent. As temperature and pH increase the concentration of $NH_3(g)$ increases. The pH of the solution depends on the type of soil, the exposure of the manure to air and may change with the aging of the manure or synthetic fertilizer TAN pool. In Eghball et al. [2000] the majority of the reported measurements of pH for beef cattle feedlot manure are between 7 and 8, although in one case a pH of 8.8 was measured. The recommended pH for various crops ranges from approximately 5.8 to 7.0 depending on the crop (e.g., http://onondaga.cce.cornell.edu/resources/soil-ph-for-field-crops). For now we simply set the pH of the solution to 7 for both the synthetic fertilizer and manure TAN pools. Sensitivity to pH is explored in section 3.4.

2.2.7 Conversion of TAN to NO_3^-. The flux from the TAN pool to NO_3^- by nitrification (F_{NO3-}, g m^{-2} s^{-1}) was adapted from that derived by Stange & Neue [2009] to describe the gross nitrification rates in response to fertilization of a surface with manure or synthetic fertilizer. In particular Stange & Neue [2009] fit measured gross nitrification rates to an expression using a maximal nitrification rate r_{max}, (μg N kg^{-1} h^{-1}) modified by a soil temperature response function ($f(T)$) and a soil moisture response function ($f(M)$) [Stange and Neue, 2009]. However, since r_{max} is fit from their experimental data the dependence of the nitrification rate on the ammonium concentration is not explicitly included in the formulation of Stange & Neue [2009]. We have remedied this by setting the maximum nitrification rate (r_{max}) in the formulation of [Stange and Neue, 2009] to $1.16\ 10^{-6}$ s^{-1} consistent with the formulation in Parton et al. [2001]:

$$F_{NO3}(m/f) = \frac{2.\, r_{max} N_{water}(m/f) NH_3(g)(m/f) K_H [H^+]/K_{NH4}}{\frac{1}{f(T)} + \frac{1}{f(M)}} \qquad (12)$$

where *f(T)* and *f(M)* are functions of soil temperature and moisture and the ammonium concentration is assumed to be in equilibrium with the other forms of ammoniacal nitrogen and is thus expressed in terms of pH, K_H and K_{NH4} and NH_3(g) (m/f).

2.2.8 Nitrate. The rate of change of the nitrate pool is given by:

$$dN_{NO3}(m/f)/dt = F_{NO3}(m/f) - K_D^{NO3} N_{NO3}(m/f) \qquad (13)$$

The source of nitrate ions is nitrification from the TAN pool (see Eq. 13). Nitrate is lost to the soil nitrate pool through diffusion. Nitrate leaching is not explicitly taken into account in the current model as the diffusion of nitrate into the soil pools occurs very rapidly. The loss of nitrate through runoff and leaching can, however, occur within the CLM, but is not tracked in the current simulations. Nitrate ions diffuse significantly faster than the NH_4^+ ions because they are not subject to immobilization by negatively charged soil particles [Mitsch and Gosselink, 2007]. Diffusion rates used in this study are derived from the same formulation as assumed for the diffusion of ammonium [e.g., see Jury et al., 1983] with a different base diffusion rate. The summary of measurements given in Canter et al. [1997], where both the diffusion of ammonium and nitrate were measured in the same soil types and wetness, suggest the base diffusion rate of NO_3^- is 13 times faster than that of ammonium.

2.2.9 TAN and Manure Water pools. The evolution of the TAN manure and synthetic fertilizer water pools depends on the water added during manure or synthetic fertilizer application and the subsequent evolution of the water in the pools. The equations for the manure and synthetic fertilizer water are:

$$dN_{water}(m)/dt = s_w(m) \times \alpha_{applied}(m) - k_{relax} \times (N_{water}(m) - M_{water}) \quad (12)$$

$$dN_{water}(f)/dt = S_w(f) \times \alpha_{applied}(f) - k_{relax} \times (N_{water}(f) - M_{water}) \quad (13)$$

These equations include a source of water ($s_w(m)$ *or* $S_w(f)$) added as a fraction of the synthetic fertilizer or manure applied and a relaxation term (k_{relax}, s^{-1}) to the soil water (M_{water}, m) calculated in the CLM for the top 5 cm of soil. The value for M_{water} explicitly takes into account the modification of the water pool due to rainfall, evaporation and the diffusion of water into deeper soil layers. We assume the TAN pool equilibrates with water within the top 5 cm of the soil with a rate of 3 $days^{-1}$. The solution is insensitive to this parameter within the ranges examined of 1 to 10 $days^{-1}$ (section 3.5). The water content of manure applied to fields depends on the animal, its feedstock and on agricultural practices. Here we assume cattle manure is added as a slurry with a dry fraction of 74.23 g kg^{-1} and a nitrogen content of 1.63 g kg^{-1}, resulting in 5.67 10^{-4} m water applied per gram of manure nitrogen applied [Sommer and Hutchings, 2001]. In the case of synthetic fertilizer we assume urea is added as a liquid spread, where water added is calculated from the temperature dependent solubility of urea in water [UNIDO and FIDC, 1998].

2.3 Model spin up and forcing

Two different type of model simulations were conducted using the CLM4.5: a present day control simulation (1990-2004) and a historical simulation (1850-2000). The resolution used in these simulations is: 1.9 degrees latitude by 2.5 degrees longitude.

2.3.1 Present day control simulation. This simulation uses the manure and synthetic fertilizer input as given in Potter et al. [2010]. Forcing at the atmospheric boundary is set to the Qian et al. [2006] reanalysis for solar input, precipitation, temperature, wind and specific humidity. The simulation is run for fifteen model years (1990-2004) with the last ten years of the simulation used for analysis. The spinup period allows for the more decomposition resistant N pools to approach a steady state with respect to the loss from mechanical incorporation into the soil.

2.3.2 Historical simulation. The historical simulation uses transient forcing conditions (accounting for changes in atmospheric CO_2, nitrogen deposition, aerosol deposition and land use change forcings) and the Qian et al. [2006] atmospheric forcing dataset. Quality 6-hourly meteorological datasets for the period prior to 1948 do not exist. Therefore from 1850 to 1973 the CLM4.5 is driven by recycled meteorological data, using meteorological data from the 1948-1973 time period. During this time there is little increase in temperature: the statistically significant changes in temperature (outside of natural variability) occur after 1973. After 1973 the meteorological data is not recycled but is valid for the year applied.

The temporal distribution of manure and synthetic fertilizer application from 1850-2000 is specified by applying the temporal distribution of Holland et al. [2005] to the base values as calculated in Potter et al. [2010]. For lack of detailed information on the geography of historical manure and synthetic fertilizer we use the scaled spatial distribution from Potter et al. [2010]. We assume manure production has changed from 26.3 Tg N yr^{-1} in 1860 to 125 Tg N yr^{-1} in 2000 [Holland et al., 2005; Potter et al., 2010], but acknowledge these temporal changes are uncertain. Synthetic fertilizer was first used in the 1920s with use increasing to 62 Tg N yr^{-1} in 2000.

3. Results

3.1 Model evaluation

To evaluate model output, measurements of the percentage of applied nitrogen that was emitted as NH_3 (P_v) from literature were compared against corresponding model predictions. The model predictions are obtained from the present day control simulation. The percent-volatilized NH_3 was used as a metric because it can be compared across time irrespective of the absolute amount of nitrogen applied to the surface. To be able to compare emissions to published measurements we require field studies with published data on: nitrogen excretion rates, NH_3 emissions, ground temperature, location, and date of measurement. Given all of these requirements we found that only a small selection of publications had enough data.

For the manure emissions, 35 measurements in a range of climates (temperatures from 1.4 °C to 28 °C) and a range of livestock management methods (commercial beef cattle feedyard, dairy cow grazing on ryegrass, beef cattle grazing on ryegrass and dairy cattle grazing on pasture land) were used (Supplementary Table 1). Each P_v reported by the measurement campaign was compared against the P_v at the corresponding grid cell in the model. For the synthetic fertilizer scenario, 10 measurements in a range of latitudes (43 °S to 50 °N) over a range of land use surfaces (pasture, sown crops, turf and forest) were used (Supplementary Table 2). Each total annual P_v reported by the measurement campaign was compared against the annual P_v of the corresponding grid cell.

3.1.1 Nitrogen volatilized as NH_3 from manure. There is a general increase in P_v with temperature, in both the model and measurements (Figure 2). However, temperature is not the only factor in determining NH_3 emissions where wind speed, water availability and below ground soil properties can also effect NH_3 emission. This is particularly demonstrated by the measurements of Todd et al. [2007] at temperatures less than 5^{o} C where the measured emissions are higher than those predicted at higher temperatures [e.g., Bussink, 1992]. It is also worth noting that the model predicts the emissions of Todd et al [2007] at lower temperatures with relative success.

The agreement between measured and modeled P_v from manure appears reasonable, with an R^2 of 0.78 that is significant at the 99.9% confidence level (p-value - 1.87 x 10^{-16}). On closer inspection, the model appears to agree best with measurements made on grassland and differs considerably with measurements made by both campaigns for beef cattle feedlots in Texas, where beef cattle feedlots are commercial operations to prepare livestock for slaughter and comprise of thousands of animals contained in a pen [US EPA, 2010]. This is perhaps not surprising, as the parameterization developed here explicitly represents emissions from manure spreading as opposed to the more managed conditions in feedlots.

3.1.2 Nitrogen volatilized as NH_3 from synthetic fertilizer. The comparison between measured and modeled annual average P_v from synthetic fertilizer applied to a range of land use types appears weak with an R^2 of 0.2 that is significant at the 90% confidence level (p-value - 0.15) (Figure 3). The lowest emissions in the model and measurements tend to be associated with the higher latitudes of both hemispheres. There does not appear to be any noticeable bias with land use type where the model estimates are both higher and lower than measured values of P_v for surfaces covered in turf, pasture land and crops. The fact that the R^2 for the synthetic fertilizer measurements is lower than the R^2 of the manure measurements is potentially caused by the single application date applied in the model, where actual farming practices may differ from model assumptions.

3.1.3 Nitrogen run-off. Here we simulate the direct nitrogen runoff from the manure and synthetic fertilzer TAN pools, but do not track the resulting nitrogen flows. These flows are tracked, however, in Nevison et al. [2016] where the nitrogen runoff from manure and synthetic fertilizer pools is routed into the River Transport Model (RTM) [Dai and Trenberth, 2001; Branstetter and Erickson, 2003] within the CESM. Nevison et al. [2016] assumes denitrification occurs within the simulated rivers at a rate inversely proportional to the river depth (amounting to approximately 30% of the nitrogen inputs on average) and compares the simulated dissolved inorganic nitrogen (DIN) export at the river mouths against measurements [Van Drecht et al., 2003] following Global NEWS

[Mayorga et al., 2010]. The simulated DIN export is nearly unbiased for six identified rivers with high human impact: the Columbia, Danube, Mississippi, Rhine, Saint Lawrence and Uruguay. Explicit comparisons against the Mississippi River show that the amplitude and seasonality of the simulated N_r runoff is in reasonable agreement with the measurements. While the comparison in Nevison et al. [2016] gives confidence the runoff is reasonably simulated, the complications in simulating river runoff preclude tight model constraints.

3.2 Global Nitrogen Pathways: Present Day

3.2.1 Geography of Nitrogen Inputs. Global maps of nitrogen input from synthetic fertilizer and manure application during the present-day simulation are given in Potter et al. [2010] and are not repeated here. Heavy synthetic fertilizer use generally occurs in the upper Midwest of the U.S. (mostly east of 100^{o} W and north of 40^{o} N), Western Europe (mostly west of 20^{o} E and north of 40^{o} N), the Northern part of India and much of Northeastern and North Central China. High manure usage coincides with the areas of heavy synthetic fertilizer use but is more widespread extending across much of Eastern South America from 20-40^{o} S and across Africa at approximately 10^{o} N.

3.2.2 Geography of Nitrogen Losses. There are strong geographical differences in the loss pathways of nitrogen following manure or synthetic fertilizer application. The importance of the various loss pathways from the TAN pool (the amount nitrogen volatilized as NH_3, runoff, nitrified or diffused directly into the soil, Figures 4-8) is dependent on temperature, precipitation and soil moisture. In hot, arid climates, the percentage volatilized is high (Figures 4 and 5). For example, regions of high NH_3 volatilization of applied manure N_r approach 50% across the southwest U.S. and Mexico, Eastern South America, central and southern Africa, parts of Australia, and across southern Asia from India to Turkey (Figure 5). The absolute highest emissions of NH_3 from applied synthetic fertilizer and from applied manure approach 20 kg N ha^{-1} yr^{-1} over hot regions with high applications, e.g. the Indian peninsula and parts of China (Figure 4 and 5). Ammonia emissions from manure are more broadly distributed globally than those of synthetic fertilizer with high NH_3 emissions not only over the synthetic fertilizer hotspots, characterized by heavy application of both synthetic fertilizer and manure, but also over southeastern South America and central Africa. For the most part, the largest synthetic fertilizer NH_3 emissions occur during April-June reflecting the single fertilization date used in this study as calculated in the CLM for corn. While Paulot et al. [2014] also show the maximum synthetic fertilizer emissions generally occur from April-June they obtain relatively higher emissions than simulated here during the other seasons. This is likely due to differences in the assumed timing of applied synthetic fertilizer: Paulot et al. [2014] consider three different synthetic fertilizer applications for each crop as well as a wide variety of crops. The seasonal emission distribution of NH_3 emissions from manure is broader than that of synthetic fertilizer but with maximum emissions usually occurring in April-June or July-Sept. The simulated geographical and seasonal NH_3 emission distribution from manure is in broad agreement with Paulot et al. [2014].

Runoff of N_r from applied synthetic fertilizer and manure TAN pools as well as nitrification and diffusion into the soil depend on precipitation and soil moisture. High manure and synthetic fertilizer N_r run off from the TAN pools (see Figure 6-7) occur particularly across parts of China, Europe (particularly the Northern parts) and the East central U.S. The global hotspot for simulated N_r runoff from the TAN pools is China where runoff approaches 20 kg N ha^{-1} yr^{-1} for nitrogen applied as either manure or synthetic fertilizer. In general the importance of runoff as a nitrogen loss pathway becomes more important in the wetter and cooler regions. In contrast, over India and Spain the agricultural nitrogen input is high, but the runoff is relatively low. In these regions with their high temperatures (and dry conditions) the NH_3 volatilization is the preferred pathway for nitrogen losses from the TAN pool.

The percent of the TAN pool nitrified or diffused directly into the soil (see Figs 7 and 8) also tends to be largest in wetter and cooler regions. The amount of nitrogen nitrified has an optimal temperature of 28^o C and tends to occur more rapidly under moist conditions; the diffusion of nitrogen into the soil is also promoted under wet conditions.

3.2.3 Regional and Global accounting of nitrogen losses. As nitrogen cascades through the environment it can be emitted as NH_3 or runoff or leached at many different stages. Here we only examine the losses directly from manure or fertilizer application. Globally, the direct loss of applied nitrogen to the atmosphere as NH_3 is similar for manure and synthetic fertilizer (17% for manure, 19% for synthetic fertilizer; see Figure 9). Our global estimates of the percent of manure and synthetic fertilizer volatilized as NH_3 are similar to Bouwman et al. [2002] and Beusen et al. [2008], although our estimate for synthetic fertilizer volatilization as NH_3 is somewhat high. Bouwman et al. [2002]

estimates 19-29% of applied manure and 10-19% of applied synthetic fertilizer volatilizes as NH_3; Beusen et al. [2008] concludes 15-23% of applied manure is lost as NH_3 (including losses from housing and storage, grazing and spreading) and 10-18% of applied synthetic fertilizer is lost.

We calculate the global direct run-off from manure or fertilizer TAN pools as 8% for manure N_r and 9% for synthetic fertilizer. Bouwman et al [2013] find that 23% of deposited N_r (comprised of synthetic fertilizer, manure and atmospheric nitrogen deposition) runs off, higher than our estimate. However, our estimate only includes the direct runoff from the TAN pool; further loss of nitrogen due to runoff and leaching may also occur from the soil nitrogen pools or downstream following NH_3 emission and re-deposition.

Our simulations assume a large fraction of emitted nitrogen is captured by the canopy, where canopy capture accounts for 25.5% of manure losses and 30% of synthetic fertilizer losses. The nitrogen captured by the canopy may have a number of fates. First, Sparks [2008] posits that since foliar nitrogen uptake is a direct addition of N to plant metabolism it could more readily influence plant growth than uptake from soils. As such it would decrease plant demand on soil uptake and thus conserve the soil nitrogen reservoirs. Secondly, nitrogen uptake by the plants, even if not directly used in plant metabolism, may redeposit onto the surface with litter fall. Finally, it may be emitted back to the atmosphere from plants. The latter process can be represented through a compensation point model between the atmosphere, the ground and stomata [e.g., Massad et al., 2010]. A full accounting of this requires the simulation to be fully coupled with the atmosphere and soil chemistry and biogeochemistry which is beyond the scope of the present study.

In the case of synthetic fertilizer the direct diffusion of TAN N_r into the soil pool (22%) is larger than nitrification (17%); for manure it is just the opposite: the nitrification (29%) is larger than the direct diffusion (14%) (Figure 9). In practice, as simulated here, this makes little difference as the diffusion of nitrate into the soil pool occurs very rapidly, an order of magnitude faster than the diffusion of nitrogen from the TAN pool. Thus NO_3^- is directly incorporated into the soil nitrate pool without any subsequent loss. Recall, also, a small percentage of manure is mechanically stirred into the soil organic nitrogen pools. Accounting for the N_r diffused from the TAN pool into the soil pools, and assuming the NH_3 emissions captured by the canopy, as well as the ammonium nitrified to NO_3^- also end up in the soil pools we find that globally 75% of manure nitrogen and 71% of synthetic fertilizer nitrogen ends up in the soil nitrogen or soil organic nitrogen pools. Of course, once in these soil pools there may be subsequent losses of nitrogen due to runoff and leaching or emissions, but these are not calculated in this initial study.

The global percentages given above change appreciably when examined over subsets of countries (Figure 10). For example, over all developed countries the percentage of emissions of manure and synthetic fertilizer TAN as NH_3 [13%] is substantially smaller than for developing countries [21%]. These differences can be largely explained by the fact that developing countries tend to be located in warmer climates than developed countries. Bouwman et al. [2002] took these differences into account when developing emission factors for developing and industrialized countries. Bouwman [2002] calculated NH_3 emission factors for manure of 21% and 26% for developed and industrialized countries, respectively and for synthetic fertilizer of 7% and 18%, respectively.

In our simulations 16% and 9% of applied agricultural nitrogen is emitted as NH_3 in the US and the European Union, respectively. The direct runoff of nitrogen accounts for 9% and 14% of the losses of agricultural nitrogen in the US and the European Union, respectively. Nitrogen runoff is favored in the cooler moister climate of Europe. However, note the large contrast between India and China, where for India NH_3 emissions are 27% of the applied N_r with very little runoff, whereas for China the runoff and emissions are approximately equal (13% and 10%, respectively).

3.2.4 Comparison to other emissions inventories. Figure 11 gives a comparison of manure and synthetic fertilizer NH_3 emissions from the FAN process model for 2000 and various bottom-up emission inventories. The bottom-up inventories rely on emission factors depending on animal husbandry, types of synthetic fertilizer usage and other details of agricultural practices. Only the NH_3 emission inventory of Huang et al. [2012] for China and Paulot et al. [2014] explicitly account for temperature to modify their emission factors; the inventory of Paulot et al. [2014] also uses wind speed to modify the emission factors. The inventories of Paulot et al. [2014] for 2005-2008, Beusen et al. [2008] for 2000, and EDGAR v4.2 for 2005-2008 are global inventories. The EDGAR inventory does not strictly separate the NH_3 emissions into those from manure and synthetic fertilizer so we simply show the overall NH_3 emissions. Over the US we also give an estimate for synthetic fertilizer NH_3 from 1995 [Goebes et al., 2003] and for NH_3 emissions from animal agricultural operations [US EPA, 2006]. Over China the global NH_3 emission estimates are supplemented by Huang et al. [2012] for 2006 and Streets et al. [2003] for 2000. Over Europe results using the Greenhouse Gas and Air Pollution Interactions and Synergies [GAINS] model are given [Klimont and Brink, 2004] as reported in Paulot et al. [2014].

Globally all inventories give approximately the same overall NH_3 emissions of 30-35 Tg N yr^{-1}. The global apportionment of emissions between manure and synthetic fertilizer in this study in approximately the ratio of 2:1, roughly consistent with that of Paulot et al. [2014] and Beusen et al. [2008]. The European and Chinese NH_3 emissions estimated here are on the low side of the other inventories, while the U.S. emissions are on the high side. In Europe the current parameterization underestimates the manure emissions compared to the other estimates, while the synthetic fertilizer emissions are on the low side. The EDGAR emissions are somewhat higher than the other estimates over Europe, although may depend on exactly what is assumed for the European boundary.

In the U.S. the manure NH_3 emissions are close to the estimate of other inventories while the synthetic fertilizer emissions are high. In China our synthetic fertilizer emissions are similar to those of Huang et al. [2012], but underestimate the manure NH_3 emissions of other inventories. Of the three regions examined all inventories suggest the Chinese emissions are highest. Note, however, there is considerable variation amongst the

Chinese inventories for both synthetic fertilizer and manure. Our results appear to match those of Huang et al. [2012] the best.

3.2.5 Site specific simulated pathways. The hourly time series of the fate of applied nitrogen from manure and synthetic fertilizer at a single site better illustrates the relationship between the different pathways and the local meteorology (Fig. 12). The large fluctuations in the NH_3 emissions and the resultant implications for atmospheric chemistry also demonstrate the desirability of inventories that respond on hourly timescales to meteorological conditions. The site shown in Fig. 12 is near the Texas panhandle. It experiences several large rain events and surface temperatures ranging from 0 to 18 ^{o}C over a period of about two months during the spring season. The response of the NH_3 emissions to the diurnal temperature range is clearly evident. The nitrogen losses of manure TAN due to NH_3 volatilization is initially small at the beginning of the examined period, on par with the diffusive loss and somewhat less than the loss due to nitrification. The loss by nitrification and diffusion from the TAN manure pool remain roughly constant through the period examined although both processes show some response to precipitation. Note in particular the diffusive loss reaches a maximum near May 21 presumably due to the increased water content in the soil by the prior rain event. With the rise in temperatures towards the end of the period, the emission loss of manure TAN becomes the dominant loss pathway and the TAN manure pool decreases. Closer inspection suggests, however, that the large increase in the NH_3 emissions towards the end of the period cannot solely be attributed to temperature, but must also be attributed to decreased water in the TAN pool as the soil dries. The latter process increases the concentration of nitrogen species within the TAN pool. The TAN manure pool is punctuated by sharp decline events, associated with precipitation and increased runoff (Fig. 12c). Synthetic fertilizer TAN responds similarly during these events but the different temporal distribution of N application for synthetic fertilizer is clearly evident in these figures. The decrease in the synthetic fertilizer TAN pool occurs on a timescale of approximately a week, consistent with the timescale used in the MASAGE_NH3 model [Paulot et al., 2014].

3.3 Global Nitrogen Pathways: Historical

Historical nitrogen pathways are accessed since 1850 in a simulation with changing climate and changing application amounts. These simulations do not include changing agricultural practices such as changes in animal housing and storage, changes in animal diet and explicit changes in land use, all of which may substantially alter the nitrogen pathways. Thus the results must be treated with caution.

The nitrogen produced as manure increases in the historical simulation from 21 Tg N yr^{-1} in 1850 to 125 Tg N yr^{-1} in 2000 (Figure 13). In 1900 we estimate that 37 Tg N yr^{1} of manure is produced, similar to the Bouwman et al (2011) estimate of 35 Tg N yr^{-1}. Emissions of NH_3 from applied manure increase from approximately 3 Tg N yr^{-1} in 1850 (14.3% of the manure produced) to 22 Tg N yr^{-1} in 2000 (17.6% of the applied manure). On the other hand the percentage of manure nitrogen that is nitrified decreases from 33 to 27% since the preindustrial. Note that the year 2000 emissions in the historical simulation differ slightly from the results of the present day control for which we report the 1995-2004 average emissions for the year 2000.

Synthetic fertilizer nitrogen application has increased dramatically since the 1960s with an estimated 62 Tg N yr^{-1} applied as synthetic fertilizer in 2000. We estimate the volatilization of synthetic fertilizer as NH_3 is 12 Tg N yr^{-1} in 2000 (19% of that applied). The percent of synthetic fertilizer nitrogen volatized to the atmosphere as NH_3 in 1920 was 8%. On the other hand, the percentage of synthetic fertilizer that is lost through runoff decreased since the preindustrial by 8%. It is evident that these percentage changes can be explained by the fact the runoff of synthetic fertilizer acts to completely drain the TAN synthetic fertilizer pool in when the application rate is small.

In part the historic emission increases in NH_3 can also be explained by changes in climate. The globally average has warmed by approximately 1^{o} C since the preindustrial. In a sensitivity experiment the temperature was artificially increased by 1^{o} C in the rate equations governing the nitrogen pathways following manure and synthetic fertilizer application. Under current manure and synthetic fertilizer application rates we find a global sensitivity of an additional 1 Tg NH_3 is emitted from the manure and synthetic fertilizer pools per degree of warming. The resulting manure emissions increase by 4% and the fertilizer emissions by 3%.

3.4 Sensitivity Tests

We have conducted a large number of sensitivity tests to evaluate the effect of changes in individual model parameters on NH_3 emissions. The various parameters may co-vary, of course, with non-linear impacts on the NH_3 emissions; however, we have not attempted to evaluate these effects. The sensitivity tests for manure are given in Table 1, those for synthetic fertilizer in Table 2. The sensitivity tests are labeled with a number denoting the sensitivity parameter perturbed and a letter denoting whether the test is with respect to manure emissions (m) or synthetic fertilizer emissions (f). In each case we give the percent change in NH_3 emissions due to the parameter change and the relative emission change with respect to the relative parameter change (the sensitivity). Rationale for the assumed parameter bounds is given in the supplement.

Except for changes in the canopy capture parameter (EX8m/f, EX9m/f) and changes in the timing or composition of manure or synthetic fertilizer inputs (EX18m, EX19f, EX20f, EX21f), changes in the sensitivity parameters directly change the nitrogen cycling within the TAN pool (as described below). For the most part the synthetic fertilizer and manure TAN pools respond similarly to the parameter changes. Note also, that except for EX18, where the amount of nitrogen input into the TAN pools is reduced, the total input and loss of nitrogen from the TAN pools remain the same for all sensitivity experiments. In general, the sensitivity of NH_3 emissions to the imposed parameter changes are within the range of $\pm$ 20% with many processes within the range of $\pm$10%. The sensitivity to the mechanical mixing of manure (EX1m, EX2m), the adjustment timescale for the water pool (EX3, EX4), the diffusion rate into the soil (EX14, EX15), the assumed depth of the water pool (EX12, EX13) and the maximum nitrification rate

(EX16, EX17) all impact NH_3 emissions by less than 20%. The sensitivity to the assumed background NH_3 concentration is also low (EX10, EX11).

The NH_3 emissions are most sensitive to changes in pH (EX5m/f, EX6m/f, EX7m/f). The NH_3 emissions decrease by approximately 60% when the pH is increased from 7 to 8 and increase by 50 to 70% (for manure and synthetic fertilizer, respectively) when the pH is decreased from 7 to 6. We also test the sensitivity of the emissions to the spatially explicit pH from ISRIC-WISE dataset [Batjes, 2005], with a global pH average of 6.55. The spatially explicit pH changed the manure NH_3 emissions by 23% and the synthetic fertilizer NH_3 emissions by 14%. Changes in pH also have a large impact on nitrification. Increased pH reduces $NH_4^+(aq)$ and thus the rate of conversion of $NH_4^+(aq)$ to NO_3^-. The effect of pH on the rate constant for nitrification is not included in the current parameterization. Parton et al. (2001) suggests this effect is small, between a pH of 6 and 8, varying only on the order of 15%. Changes in pH also result in marked changes in the runoff and soil diffusion due to the large changes in emissions and nitrification: low pH's act to increase the flux of nitrogen through these loss pathways, high pH's act to decrease them.

Emissions are also highly sensitive to changes in canopy capture (i.e., the parameter *fcapture)* as shown in EX8m/f, EX9m/f. Decreasing the fraction captured by the canopy by a factor of 2 increases the emissions by approximately a factor of 3. Changes in this fraction modify the fixed ratio between the amount of nitrogen captured by the canopy and that emitted to the atmosphere. Of course, the nitrogen captured in the canopy impacts the overall soil nitrogen budget, but this impact is not simulated here.

The NH_3 emissions are somewhat sensitive to the depth of the assumed water pool (EX12m/f, EX13m/f). Smaller depths (less water) give higher concentrations of all the constituents within the TAN pool resulting in higher NH_3 emissions (equations 7 and 11) and larger nitrogen runoff (section 2.4.1). Larger depths (more water) have the opposite effect. The diffusion of nitrogen into the soil is somewhat sensitive to changes in the assumed water depth as the coefficient of diffusion is proportional to the water content to the 10/3 power (see appendix).

We conducted various sensitivities to synthetic fertilizer applications. Early synthetic fertilizer applications decrease NH_3 emissions due to their strong temperature dependence and increase the susceptibility of the TAN pool to washout. An early fertilization date (set to March 15) decreases the NH_3 emissions by 23% and increases the nitrogen run off from the TAN pool by 62% (EX19f). To investigate the sensitivity to the application rate of synthetic fertilizer, synthetic fertilizer was applied over 20 days as opposed to the single day application assumed in the default version (EX20f). This did not have a significant impact on the emissions. The assumed synthetic fertilizer type in the default version of the model (urea) was replaced with ammonium nitrate fertilizer in EX21f. Whereas urea is converted to NH_3 rather slowly, the conversion of ammonium nitrate is rapid (in the sensitivity test it is assumed to be instantaneously released into the TAN pool and result in no changes in pH). However, the emissions are not particularly sensitive to this change. This is in contrast to differences in volatilization rates of different synthetic fertilizers given in Bouwman (2002). Whitehead and Raistrick (1990) show that one of the primary differences between the addition of urea versus ammonium nitrate as fertilizer is in the effect of the fertilizer on the soil pH, an effect that we do not consider in this first study. In particular urea increases the soil pH and thus the NH_3 emissions.

Finally we test the impact of manure composition on the NH_3 emissions (EX18f). The composition of manure nitrogen excreted by animals depends in part on the digestibility of the feed, which can vary in both time and space. To investigate this uncertainty we varied the composition of the manure assumed in the default model version (50% urine, 25% available, 22.5 % resistant and 2.5% unavailable) to the less soluble N excreta from dairy cattle in sensitivity simulation EX18m (41% urine, 21% available, 25% unavailable and 13% resistant [Smith, 1973]). This decreased the NH_3 emissions by 21 percent.

It is important to emphasize that these sensitivity simulations only test the parameter sensitivity within the imposed model. In particular, the sensitivities to various farming practices are generally extraneous to the model assumptions with some exceptions. The sensitivities to synthetic fertilizer or manure input assumptions are tested in simulations EX18m, EX19f, EX20f, EX21f; sensitivities to the water depth which may crudely represent some of the impacts of plowing manure or synthetic fertilizer into the soil are examined in EX12 and EX13; finally modifications to soil pH are tested in EX5, EX6 and EX7.

4. Discussion and Conclusions

In this paper we develop a process-oriented model that predicts the climate dependent reactive nitrogen pathways from synthetic fertilizer and manure application to the surface of the land. Continued population growth will likely result in an increased application of synthetic fertilizers with concurrent increases in manure production in the future [Davidson, 2012]. Climate is an important determinant in the ultimate fate of this applied nitrogen, important in determining the resulting emissions of NH_3 and other reactive nitrogen gases, in the runoff of the applied nitrogen, its nitrification and its incorporation into the soil organic and inorganic pools. The fate of the resultant applied nitrogen may act to acerbate climate change through the formation of N_2O, or perhaps mitigate climate change through increased carbon fertilization and the increased formation of aerosols. On the flip side the impact of a changing climate on agriculture and the resultant pathways for N_r is likely to be significant.

Agricultural NH_3 emissions are an unusual emission source in that both natural and anthropogenic processes control their emissions. Previous global NH_3 emission inventories have exclusively used bottom up emission factors mainly governed by agricultural practices. In many cases the emission factors only implicitly include temperature dependence by using different emission factors for industrial and developing countries [e.g., Bouwman et al. 1997], although recently some inventories have included empirical emission factors that vary with temperature [Paulot et al., 2014; Huang et al., 2012]. Here, however, we take the opposite tact by constructing a model where the N_r pathways and in particular the NH_3 emissions are explicitly driven by climate but where the explicit representation of most agricultural practices is minimized. We find the global emissions of NH_3 due to manure and fertilizer nitrogen sources are similar to other recent inventories, with 21 Tg N yr^{-1} emitted from manure nitrogen and 12 Tg N yr^{-1} emitted from synthetic fertilizer. Strong regional differences in emissions captured by the bottom up inventories are also simulated. Moreover, we are able to simulate the inter-annual, seasonal and diurnal changes in NH_3 emissions critical for air pollution applications [e.g., see De Meij et al., 2006]. Most previous inventories have included no seasonal dependence of the emissions, although in some cases a seasonal dependence is empirically introduced. It is perhaps important to note that the impact of nitrogen emissions on the global carbon budget has generally made use of these previous inventories without explicit seasonal or diurnal dependence of NH_3 emissions and with a rather minimal representation of the geographic meteorological dependence.

The model developed here uses a process level approach to estimate nitrogen pathways from fertilizer and manure application. It is suitable for use within an Earth System model to estimate the resulting NH_3 emissions, nitrogen run-off, and the incorporation of the nitrogen into soil organic and inorganic matter. The modeled N_r pathways dynamically respond to climatic variation: (1) the breakdown timescale of manure and fertilizer into TAN depends on temperature; (2) the formation of NH_3 gas from the TAN pool is highly temperature sensitive with the rate of formation described by the temperature dependence of the thermodynamic Henry and dissociation equilibria for NH_3 [Nemitz et al., 2000]; (3) the rate of nitrification of NH_3 within the TAN pool, determined by the rate at which ammonium ions are oxidized by nitrifying bacteria to form nitrate ions [Abbasi and Adams, 1998] is controlled by environmental factors such as soil temperature and soil moisture; (4) the runoff of N_r is determined by the precipitation. Predictions for direct nitrogen runoff from fertilizer and manure nitrogen pools and the incorporation of nitrogen into soil pools from applied fertilizer and manure nitrogen are some of the first made by a global process-level model. Measurements of nitrogen runoff from rivers heavily impacted by anthropogenic nitrogen input compare favorably with simulated results using the River Transport Model within the CESM [Nevison et al., 2016].

Manure is not a new nitrogen source, but contains recycled N_r from soil nitrogen produced when animals eat plants. Therefore to conserve nitrogen within an earth system model, the application of manure determines the consumption of plant matter by animals. Specifically, the model calculates the amount of nitrogen and carbon needed for a given manure application and subtracts it from the plant leaf pools within the CLM. The manure production acts to speed up the decay and processing of plant biomass, releasing different N_r products to the atmosphere than natural decay [Davidson, 2009].

The climate dependency incorporated into the model suggests that the pathways of nitrogen added to the land are highly spatially and temporally heterogeneous. An examination of nitrogen loss pathways at a point over Texas shows the variation of the nitrogen pathways on a variety of timescales with changes in temperature, precipitation and soil moisture. Spatially, values for the percentage of manure nitrogen volatilized to NH_3 in this study show a large range in both developing countries (average of 20% (maximum: 36 %)) and industrialized countries (average of 12% (maximum: 39 %)). The model also predicts spatial and temporal variability in the amount of NH_3 volatilized as manure from agricultural fertilizers ranging from 14% [maximum 40 %] in industrialized countries to 22 % [maximum 40 %] in developing countries. As a result of temperature dependency, NH_3 volatilization is highest in the tropics with largest emissions in India and China where application of fertilizer and manure is high. In comparison, the EDGAR database uses the emission factors based on Bouwman et al. (2002), where 21 % and 26 % of manure is converted into NH_3 in industrialized and developing countries, respectively. The respective emission factors for fertilizer application calculated here are 7 % in industrialized countries and 18 % in developing countries. Nitrogen run-off from the manure and synthetic fertilizer TAN pools is highest in areas of high N_r application and high rainfall, such as China, North America and Europe. Despite high nitrogen input rates we simulate low nitrogen runoff in India and Spain, for example. We also simulate climate dependent pathways for the diffusion of N_r into the soil inorganic nitrogen pools and the nitrification of ammonium to nitrate.

Historically we predict emissions of NH_3 from applied manure to have increased from approximately 3 Tg N yr^{-1} in 1850 to 22 Tg N yr^{-1} in 2000 while the volatilization of fertilizer reaches 12 Tg N yr^{-1} in 2000. The NH_3 emissions increase by approximately 4% for manure applications and 5% for fertilizer applications over this historical period

(1930 to 2000 for fertilizer). Under current manure and synthetic fertilizer application rates we find a global sensitivity of an additional 1 Tg NH_3 is emitted from the manure and synthetic fertilizer pools per degree of warming. The resulting manure emissions increase by 4% and the fertilizer emissions by 3%. Increases are not evident in the runoff of nitrogen. Note, however, we do not include runoff and leaching from the mineral nitrogen pools within the CLM in these calculations. The latter may be impacted by plant nitrogen demand such that excess fertilization would act to increase the nitrogen runoff.

The NH_3 emissions appear reasonable when compared to other inventories on the global scale, but also when compared to the local scale measurements of manure and synthetic fertilizer (Figure 2 and 3), although these latter comparisons highlight the difficulty in making global scale assumptions about surface parameters and farming methodology. The biggest disagreement with the manure emission measurements is from beef cattle feedlots in Texas. On the whole the model performs best when estimating NH_3 manure emissions from cows on grassland. Despite the issues described above, this model gives reasonable NH_3 emission predictions given the limited global information available on the grazing land of agricultural animals.

The model described here is capable of predicting global to regional impacts of climate on applied synthetic fertilizer and manure nitrogen. It is also capable of taking into account the resulting biogeochemical cycling of nitrogen. Previous estimates of NH_3 emissions have relied on detailed information on animal type, animal housing if any and the field application of synthetic fertilizer or manure [e.g., Bouwman et al., 1997] but have minimized the representation of meteorological processes. These estimates have also not allowed for an explicit representation of the biogeochemical nitrogen cycling and loss pathways. Here we take the opposite tact by taking into account the importance of meteorological variability in accounting for regional and temporal differences in NH_3 emissions and nitrogen cycling. However, we have greatly simplified agricultural management practices. The use of simplified farming practices may be acceptable in many locations as more complex farming methods are rarely employed in the developing world. The Food and Agriculture Organization [FAO, 2005] suggests over 75 % of the global agricultural land uses traditional farming methods. Nevertheless, one of the largest sources of uncertainty in this study is associated with the simplification of agricultural practices. This FAN model uses a single date for synthetic fertilizer application, considers only urea fertilizer, and does not take into account manure storage methods, such as slurry pools or different types of animal manures. It also assumes a fixed depth of manure and synthetic fertilizer application. The truth of course lies somewhere between: both meteorological variability and a detailed accounting of management practices is necessary to fully account for nitrogen cycling from agricultural practices and the resulting NH_3 emissions.

A number of future model improvements are necessary in the next generation model. (1) More realistic representation of manure mangement practices. Globally, somewhat over 40% of manure is excreted in animal houses and stored prior to being spread onto fields. While there is a wide range of variation in animal housing and storage practices, the unique set of emission factors entailed in animal housing and storage should be incorporated in the next model generation. (2) A better representation of nitrogen transport throughout the soil column and the resulting NH_3 generation. This would allow a differentiation between NH_3 emissions resulting from grazing, where urine is rapidly incorporated into the soil column, versus emissions resulting from the spreading of manure slurry. It would also allow a representation of fertilizer injection or mixing into the soil column and the transport of nitrogen into the soil column in association with water transport. (3) Representation of NH_3 emissions from different synthetic fertilizer formulations. Different types of synthetic fertilizer have rather different emission factors. As shown by Whitehead and Raistrick [1990] many of these differences can be represented by the impact of the fertilizer on soil pH. (4) A full biogeochemical coupling of the FAN process model to the overall biogeochemistry within the CLM. This would allow the nitrogen introduced through agricultural practices to impact the overall model biogeochemistry and allow a more thorough investigation of the flows of agricultural nitrogen. Here the fertilizer nitrogen would be added explicitly to the CLM crop model where appropriate. (5) A full coupling between the NH_3 emissions represented by the FAN process model and the atmospheric chemistry model through a PFT-dependent compensation point approach. In this approach the atmospheric model would directly provide the nitrogen deposition fields to the land model.

The increased use of synthetic fertilizer and growing livestock populations has increased N_r emission to both the atmosphere and oceans to unprecedented levels with a marked effect on the environment. We have provided a first estimate of globally distributed temporal changes in nitrogen pathways from manure and synthetic fertilizer inputs in response to climate. This is relevant to current studies investigating the ecosystem effects of N_r, and in particular, how adding synthetic fertilizer to farmland affects the ocean, the atmosphere and impacts climate. The model predicts vastly different nitrogen pathways depending on the region the inputs are applied. Scenarios predicting future synthetic fertilizer use and livestock populations suggest large increases in nitrogen added to the land surface from both sources [Tilman et al., 2001; Skjoth and Geels, 2013]. The climate dependence of the nitrogen pathways suggests these pathways will be sensitive to climate change. The interaction of these changes with climate is not yet clear. The volatilization of NH_3 increases exponentially with temperature suggesting future increases are likely. However, increases in temperature may surpass the optimal temperature at which certain biological processes occur, slowing the process. Washout pathways are also likely to change, not only with climate, but with increases in nitrogen loading. Future applications of this model will investigate the tight coupling between nitrogen, agriculture and climate.

Acknowledgments

We wish to thank the reviewers. Also, Farhan Nuruzzaman and Jae Hee Hwang for preparation of input datasets. Thanks also to Sam Levis, Dave Lawrence and Gordon Bonan at NCAR for their input to model processes and colleagues at Cornell University, Ben Brown-Steiner and Raj Paudel, for their help running the model. This project was supported by NSF Project number ETBC #10216.

Appendix A. Description of Model Variables and Equations.

Description	Symbol	Unit	Value Used or Equation	Reference
<u>Prognostic Variables</u>				
Pool of nitrogen from applied manure that easily forms TAN	$N_{available}$	g m^{-2}	$dN_{available}/dt =$ $f_a \; x \; \alpha_{applied}(m)$ $- K\_a \cdot N_{available} - k\_m \cdot N_{available}$	
Pool of nitrogen from applied manure that is resistant to forming TAN	$N_{resistant}$	g m^{-2}	$dN_{resistant}/dt =$ $f_r \; x \; \alpha_{applied}(m) - K\_r \cdot N_{resistant} - k\_m$ $\cdot N_{resistant}$	
Pool of nitrogen from applied manure that does not form TAN	$N_{unavailable}$	g m^{-2}	$dN_{unavailable}/dt =$ $f_{un} \; x \; \alpha_{applied}(m) - k\_m \cdot N_{unavailable}$	

Pool of nitrogen from applied fertilizer	$N_{fertilizer}$	g m^{-2}	$dN_{fertilizer}/dt =$ $\alpha_{applied}(f)$ $-k\_f \cdot N_{fertilizer}$	
Pool of nitrogen in TAN pool from manure	$N_{TAN\ (m)}$	g m^{-2}	$N_{TAN}\ (m)/dt =$ $f_u x\ \alpha_{applied}$(m) $+ K\_r \cdot N_{resistant}$ $+K\_a \cdot N_{available}$ $-K\_w \cdot N_{TAN}(m)$ $-K_D^{NH4} \cdot N_{TAN}(m)$ $-\ F_{NH3}\ (m)$ $-\ F_{NO3}(m)$	

Pool of nitrogen in TAN pool from fertilizer	$N_{TAN\,(f)}$	g m^{-2}	$N_{TAN}\,(f)/dt =$ $+\,k\_f \cdot N_{fertilizer}$ $-K\_w \cdot N_{TAN}(f)$ $-K_D^{NH4} \cdot N_{TAN}(f)$ $-\,F_{NH3}(f)$ $-\,F_{NO3}(f)$	
Pool of surface NO_3^-	N_{NO3}	g m^{-2}	$dN_{NO3}\;/dt =$ $F_{NO3}(m/f) - K_D^{NO3} \cdot N_{NO3}$	
Pool of manure/fertil-izer water in TAN pool	$N_{water}\,(m)$	m	$dN_{water}\,(m)/dt =$ $s_w(m) \times \alpha_{applied}(m))$ $-k_{relax} \times (N_{water}(m) - M_{water})$	

Pool of manure/ fertilizer water in TAN pool	$N_{water}\ (f)$	m	$dN_{water}\ (f)/dt =$ $S_w(f)\times\alpha_{applied}(f))$ $-k_{relax}\times(N_{water}(f) - M_{water})$	
<u>Variables from CLM</u>				
Ground Temperature	T_g	^{o}K	Taken from model	
Run-off	R	m s^{-1}	Taken from model	
Aerodynamic resistance	R_a	s m^{-1}	Taken from model	
Boundary Layer resistance	R_b	s m^{-1}	Taken from model	
Water in soil	M	m	Taken from the model (top 5 cm of soil)	

Diagnostic Variables				
Available manure decomposition	K_a	s^{-1}	$K\_a = k_{a1}\, T_R(T_g)$	[Gilmour et al., 2003; Vigil & Kissel, 1995]
Resistant manure decomposition	K_r	s^{-1}	$K\_r = k_{a2}\, T_R(T_g)$	[Gilmour et al., 2003; Vigil & Kissel, 1995]
Temperature dependence for K_a, K_r	T_R	N/A	$T_R(T_g) = t_{r1} \exp\left(t_{r2}\left(T_g - 273.\right)\right)$	[Vigil & Kissel, 1995]
Surface runoff flux	$F_{run}(m/f)$	g $m^{-2}s^{-1}$	$F_{run}(m/f) = R \cdot \frac{N_{TAN}(m/f)}{N_{water}(m/f)}$	
NH_4^+ loss rate to soil pool	K_D^{NH4}	s^{-1}	$K_D^{NH4} = (1/l^2) \cdot (\Theta_w^{10/3} / \varphi^2)\varkappa_{NH4}^{aq}$	[Génermont and Cellier, 1997]
NO_3^- loss rate to soil pool	K_D^{NO3}	s^{-1}	$K_D^{NO3} = (1/l^2) \cdot (\Theta_w^{10/3} / \varphi^2)\varkappa_{NO3}^{aq}$	[Génermont and Cellier, 1997]

Base vertical diffusion for TAN pool	$\varkappa_{NH4}^{aq}$	m^2s^{-1}	$\varkappa_{NH4}^{aq} = 9.8\ 10^{-10} \cdot 1.03^{(T_g - 273.15)}$	[Génermont and Cellier, 1997]
Base vertical diffusion for NO3 pool	$\varkappa_{NO3}^{aq}$	m^2s^{-1}	$\varkappa_{NO3}^{aq} = 1.3\ 10^{-8} \cdot 1.03^{(T_g - 273.15)}$	[Génermont and Cellier, 1997]
Water Content	Θ_w		$\Theta_{w=} N_{water}(m/f)/\mathcal{H}$	
Flux of nitrogen lost as NH_3 for manure(m) or fertilizer(f)	$F_{NH3}(m/f)$	$g\ m^{-2}\ s^{-1}$	$F_{NH3}(m/f) = \dfrac{NH_3(g)(m/f) \quad - \chi_a}{(R_a(z) + R_b)}$	[Nemitz et al., 2000; Loubet et al., 2009; Sutton et al., 2013]]
Flux of NH3 to atmosphere	${F_{NH3}}_{atm}$ (m/f)	$g\ m^{-2}\ s^{-1}$	${F_{NH3}}_{atm}(m/f) = (1 - f_{capture}\ ) \times F_{NH3}(m/f)$	[e.g., Wilson et al., 2004]

NH3(g) in equilibrium with the TAN manure (m) or fertilizer (f) pool	$NH_3\ (g)$ (m/f)	g m^{-3}	$NH_3\ (g)(m/f) = \dfrac{N_{TAN}\ (m/f)/\ N_{water}(m/f)}{1 + K_H +\ K_H[H^+]/K_{NH4}}$	Derived from [Sutton et al., 1994]
Henry's Law Constant for NH_3	K_H		$K_H\ = 4.59\ (\ {}^oK^{-1}) \cdot T_g \cdot exp^{4092(1/T_g - 1/T_{ref})}$	[Sutton et al., 1994]
Dissociation Equilibrium Constant for $NH_3\ (aq)$	K_{NH4}	mol l^{-1}	$K_{NH4}\ = 5.67\ 10^{-10} exp^{-6286(1/T_g - 1/T_{ref})}$	[Sutton et al., 1994]
Flux of nitrogen from TAN to NO_3^- pool	$F_{NO3}(m/f)$	g m^{-2} s^{-1}	$F_{NO3}(m/f) = \dfrac{2.\ r_{max}N_{water}(m/f)xNH_3\ (g)(m/f)K_H[H^+]/K_{NH4}}{\frac{1}{\Sigma(T_g)} + \frac{1}{\Pi(M)}}$	[Stange and Neue, 2009, Parton et al., 2001]

Soil temperature function	$\Sigma\ (T_g)$		$\Sigma(T_g) = \left(\frac{t_{max} - T_g}{t_{max} - t_{opt}}\right)^{a\ \Sigma} exp\left(a_{\ \Sigma}\left(\frac{T_g - t_{opt}}{t_{max} - t_{opt}}\right)\right)$	[Stange and Neue, 2009]
Soil moisture response function	$f(M)$		$\Pi(M) = 1 - e^{-\left(^{[(M\cdot\rho_{water})/(h\cdot\rho_{soil})]}/_{m_{crit}}\right)^{b}}$	[Stange and Neue, 2009]
Water:N ratio in applied fertilizer	$S_w(f)$	m^3g^{-1}	$S_w(f) = \frac{1\cdot 10^{-6}}{0.466\times 0.66\times e^{0.0239\times(T_g-273)}}$	[UNIDO and FIDC, 1998]

Parameters				
Flux of manure nitrogen applied to the surface	$\alpha_{applied}(m)$	g m^{-2} s^{-1}	Spatial distribution from Potter et al. (2010); annual temporal distribution from Holland et al. (2005)	[Potter et al., 2010; Holland et al., 2005]
Flux of fertilizer nitrogen applied to the surface	$\alpha_{applied}(f)$	g m^{-2} s^{-1}	Spatial distribution from Potter et al. (2010); annual temporal distribution from Holland et al. (2005)	[Potter et al., 2010; Holland et al., 2005]
Fractions of nitrogen in manure/urine	f_u, f_a, f_r, f_{un}	N/A	$f_u = 0.5$, $f_a = 0.25$, $f_r = 0.225$, $f_{un} = 0.025$	[Gusman and Marino, 1999]
Mechanical incorporation of manure into soil	k_m	s^{-1}	$k\_m = (365*86400)^{-1}$	see Koven et al. [2013]

Fertilizer Decomp-osition	k_f	s^{-1}	$k\_f = 4.83 \times 10^{-6}$	[Agehara and Warncke, 2005]
Water:N ratio in applied manure	$s_w(m)$	$m^3 g^{-1}$	$s_w(m)$=5.67 10^{-4}	[Sommer and Hutchings, 2001]
Relaxation rate of TAN water pool to soil water pool	k_{relax}	s^{-1}	$k_{relax} = (3*86400)^{-1}$	
Empirical factors for K_a, K_r	k_{a1}, k_{a2}	s^{-1}	$k_{a1} = 8.94 \times 10^{-7}\ s^{-1}$, $k_{a2} = 6.38 \times 10^{-8}\ s^{-1}$	[Gilmour et al., 2003]
Empirical factors for T_r	t_{r1}, t_{r2}	$^{o}K^{-1}$	$t_{r1} = 0.0106$, $tr_2 = 0.12979\ ^{o}K^{-1}$	[Vigil & Kissel, 1995]
Length Scale	l	m	$l=10^{-2}\ m$	

Soil Porosity	φ		$\varphi=0.5$	
Depth of Soil Water Pool	$\mathcal{H}$	m	$\mathcal{H} = 5.0\ 10^{-2}$	
Atmospheric NH_3 concentration	χ_a	g m^{-3}	$\chi_a = 0.3 \text{ x } 10^{-6}\text{g m}^{-3}$	[Zbieranowski and Aherne, 2012]
Fraction of ammonia emissions capture by canopy	$f_{capture}$		$f_{capture} = 0.7$	[e.g., see Wilson et al., 2004]
Concentration of Hydrogen Ions	$[H^+]$	mol l^{-1}	$[H^+] = 10^{-7}$	
Reference Temperature	T_{ref}	^{o}K	$T_{ref} = 298.15$	[Sutton et al., 1994]
Maximum rate of nitrification	r_{max}	s^{-1}	$r_{max} = 1.16\ 10^{-6}$	[Parton et al., 2001]

Optimal temperature of microbial activity	t_{opt}	K	$t_{opt} = 301$	[Stange and Neue, 2009]
Maximum temperature of microbial activity	t_{max}	K	$t_{max} = 313$	[Stange and Neue, 2009]
Empirical factor	a_{Σ}		$a_{\Sigma} = 2.4$	[Stange and Neue, 2009]
Sharp parameter of the function	b		$b = 2$	[Stange and Neue, 2009]
Critical water content of soil	m_{crit}	g g^{-1} soil	$m_{crit} = 0.12$	[Stange and Neue, 2009]
Density of soil	ρ_{soil}	kg m^{-3}	$\rho_{soil} = 1050.$	

Table 1. Manure Sensitivity Tests

Exper[1]	Parameter[2]	Value[3]	NH3[4]	Run[5]	Soil[6]	Nitrif.[7]	Canopy[8]	ΔNH3[9] %	Sens.[10] %/%
Control[11]			19.5	10.2	15.2	32.3	29.2		
EX1m	*k_m*	100 d^{-1}	16.6	9.1	13.6	41.8	24.8	-15	.20
EX2m	*k_m*	750 d^{-1}	20.8	10.7	16	25.9	31.2	+7	.06
EX3m	k_{relax}	1 d^{-1}	19.5	10.2	15.3	32.2	29.2	0	0.0
EX4m	k_{relax}	10 d^{-1}	19.4	10.3	15.2	32.4	29.1	+1	0.0
EX5m	pH	6	8.0	16.6	23.9	45.8	12.0	-59	4.1
EX6m	pH	8	29.6	3.7	5.1	23.5	44.4	+52	3.6
EX7m	pH	Dataset[12]	15.0	13.8	18.4	36.8	22.5	-23	
EX8m	$f_{capture}$	0.4	29.2	10.2	15.2	32.3	19.5	+50	-1.3
EX9m	$f_{capture}$	0.8	9.7	10.2	15.2	32.3	38.9	-50	-2.2
EX10m	χ_a	.1 ug m^{-3}	20.0	9.9	14.7	31.8	30.0	+3	-.04
EX11m	χ_a	1 ug m^{-3}	18.2	11.1	16.4	33.5	27.3	-7	-.03
EX12m	H2O Depth	10 cm	16.0	7.7	20.7	37.9	24.1	-18	-.18
EX13m	H2O Depth	2 cm	23.1	13.4	8.2	27.1	34.6	+18	-.31
EX14m	K_D	×0.5	20.7	11.6	9.4	33.8	31.0	+6	-.12
EX15m	K_D	×2.0	17.8	8.5	22.9	30.4	26.8	-9	-.09
EX16m	r_{max}	× 0.5	20.7	11.0	16.7	27.0	31.1	+6	-.12
EX17m	r_{max}	× 2.0	17.5	9.0	13.0	40.5	26.3	-10	-.10
EX18m	*manure comp*[13]		15.4	8.4	12.5	23.8	23.1	-21	

[1]Control Experiment [2]Parameter changed from default values [3]New parameter value [4]NH_3 emissions (Tg N yr^{-1}) [5]Runoff (Tg N yr^{-1}) [6]Diffusion to soil (Tg N yr^{-1}) 7Nitrification (Tg N yr^{-1}) [8] Canopy capture (Tg N yr^{-1}) [9]Percent change in NH_3 emissions due to parameter change (%) [10] Percent change in NH_3 emissions

per % change in parameter value [11]Control simulation [12] Soil pH from the ISRIC-WISE dataset [Batjes, 2005][13]Change in manure composition to urine 41%, available 21%, unavailable 25%, and resistant 13%

Table 2. Fertilizer Sensitivity Tests

Exper[1]	Parameter[2]	Value[3]	NH3[4]	Run[5]	Soil[6]	Nitrif.[7]	Canopy[8]	ΔNH3[9] %	Sens.[10] %/%
Control[11]			10.9	5.3	12.3	9.8	16.3		
EX3f	k_{relax}	1 d^{-1}	11.3	5.6	11.6	9.0	17.0	+4	-.06
EX4f	k_{relax}	10 d^{-1}	10.1	4.7	13.7	10.9	15.1	-7	-.03
EX5f	pH	6	4.4	8.5	17.7	17.5	6.5	-60	+4.2
EX6f	pH	8	18.4	1.5	4.1	2.8	27.6	+69	+4.8
EX7f	pH	Dataset[12]	9.4	6.6	13.5	10.9	14.1	-14	
EX8f	$f_{capture}$	0.4	16.3	5.3	12.3	9.8	10.9	+50	-1.2
EX9f	$f_{capture}$	0.8	5.4	5.3	12.3	9.8	21.7	-50	-2.1
EX10f	χ_a	.1 ug m^{-3}	10.9	5.2	12.3	9.8	16.3	+0	0.0
EX11f	χ_a	1 ug m^{-3}	10.8	5.3	12.4	9.9	16.1	-1	0.0
EX12f	H2O Depth	10 cm	9.0	4.0	15.2	12.9	13.4	-17	-.17
EX13f	H2O Depth	2 cm	12.9	6.8	8.3	7.2	19.3	+18	-.31
EX14f	K_D	×0.5	11.8	6.1	7.6	11.3	17.7	+8	-.17
EX15f	K_D	×2.0	9.6	4.2	18.3	7.9	14.4	-12	-.12
EX16f	r_{max}	× 0.5	11.8	5.8	13.7	5.5	17.7	+8	-.17
EX17f	r_{max}	× 2.0	9.4	4.4	10.3	16.3	14.2	-14	-.14
EX18f	*Fert. Date*[13]		8.4	8.6	15.5	8.6	12.6	-23	
EX19f	*Fert. Rate*[14]		11.3	5.6	11.5	9.1	17.0	+4	
EX20f	*Fert Decomp*[15]		10.5	4.9	12.9	10.5	15.7	-4	

[1]Control Experiment [2]Parameter changed from default values [3]New parameter value [4]NH_3 emissions (Tg N yr^{-1}) [5]Runoff (Tg N yr^{-1}) [6]Diffusion to soil (Tg N yr^{-1}) 7Nitrification (Tg N yr^{-1}) [8] Canopy capture (Tg N yr^{-1}) [9]Percent change in NH_3 emissions due to parameter change (%) [10] Percent change in NH_3 emissions per % change in parameter value [11]Control simulation [12] Soil pH from the ISRIC-WISE dataset [Batjes, 2005]. [13]Change in fertilizer date to Mar 20 (NH) and Sept 20 (SH) [14]Apply fertilizer over 20 days [15]Assume fast release ammonium nitrate decay of fertilizer

Figure Captions.

Figure 1. Schematic of the addition of manure and fertilizer (Process Model) to the CESM nitrogen cycle. Some minor pathways are not shown. Soil nitrogen pools and and plant nitrogen exist in CLM4.5. Urine nitrogen (N_{urine}) is directly input to the TAN pool while fecal matter is split into three parts that decompose into the TAN pool at a rate determined by their C: N ratio ($N_{available}$, $N_{resistant}$, $N_{unavailable}$). Manure nitrogen that does not mineralize ($N_{unavailable}$) is added to the soil organic nitrogen pool. Nitrogen applied as synthetic fertilizer is added to the $N_{fertilizer}$ pool where it decomposes into the TAN pool. Losses from the TAN pool include ammonia (NH_3) emission (into CAM-chem), nitrogen run-off (into the RTM), above ground nitrate (NO_3^-) formation and diffusion to the soil nitrogen pools.

Figure 2. Comparison of model to measurements for percentage of nitrogen lost as NH_3 emissions from manure for a range of studies (see supplementary Table 1). Symbol color measures temperature at which emissions were made; shape gives the study.

Figure 3. Comparison of model to measurements for percentage of nitrogen lost as NH_3 emissions from fertilizer (see supplementary Table 2). Symbol color gives the latitude at which the measurement was made; symbol shape gives the study and type of fertilizer application.

Figure 4. Simulated NH_3 emissions from fertilizer application from 1995-2004 for the present-day control simulation. Simulated emissions (kg N ha^{-1} yr^{-1}) as a) an annual average, c) Jan-Feb-Mar average, d) Apr-May-Jun average, e) Jul-Aug-Sep average, and f) Oct-Nov-Dec average. Simulated emissions as a percent of annual fertilizer application, b).

Figure 5. As in Figure 4 but for manure application.

Figure 6. Simulated runoff of N_r from fertilizer and manure TAN pools for the present-day (1995-2004) control simulation. Simulated runoff (kg N ha^{-1} yr^{-1}) as an annual average for a) fertilizer, c) manure. Simulated as a) percent of annual fertilizer application, d) percent of annual manure application.

Figure 7. As in Figure 6, but for simulated nitrification.

Figure 8. As in Figure 6 but for flux of TAN nitrogen to the soil.

Figure 9. Global Fate of TAN Nr applied as fertilizer (a) or as manure (b). Emissions are split between those to the atmosphere and those captured by the canopy.

Figure 10. As in Figure 9, but fate of TAN nitrogen by country and region. Countries are split between developed countries and developing countries.

Figure 11. Comparison of manure (red) and synthetic fertilizer (blue) ammonia emissions or combined manure and synthetic fertilzer emissions (green) (Tg N yr^{-1}) a**)** globally, b) China, c) Europe and d) US for this study (Riddick) and for other studies. See text for details.

Figure 12. Site specific pathways for nitrogen budget at 35˚N and 100˚W, near the Texas panhandle . Panels show a) the temperature (^{o}C) and precipitation (mm s^{-1}) used to force the CLM, b) the manure (solid) and fertilizer TAN pools (dashed) (gN m^{-2}), and the four major loss pathways from the TAN pools (NH_3 emissions, red; runoff, orange; nitrification, green; diffusion to the soil, blue) (g N m^{2} s^{-1}) from c) the manure TAN pool d) the fertilizer TAN pool.

Figure 13. Applied nitrogen and nitrogen losses for the historical simulation in Tg N yr^{-1} for a) manure and c) fertilizer. Nitrogen losses from the TAN pool as a percentage of applied nitrogen for the historical simulation for b) manure and d) fertilizer. The losses from the TAN pool are divided into emission losses of ammonia to the atmosphere (golden diamond), runoff (green diamond) and loss to the soil. Loss to the soil is divided into that due to canopy loss (askerisk) , direct diffusive loss (cross) and nitrification (plus) (see section 3.2.3).

REFERENCES

Abbasi, M. K. and W. A. Adams (1998), Loss of nitrogen in compacted grassland soil by simultaneous nitrification and denitrification, Plant Soil, 200(2), 265-277, doi:10.1023/A:1004398520150.

Adams, P. J., J. H. Seinfeld, D. Koch, L. Mickley, and D. Jacob (2001), General circulation model assessment of direct radiative forcing by the sulfate-nitrate-ammonium-water inorganic aerosol system, Journal of Geophysical Research-Atmospheres, 106(D1), 1097-1111, doi:10.1029/2000JD900512.

Agehara, S. and Warncke, D. D. (2005), Soil Moisture and Temperature Effects on Nitrogen Release from Organic Nitrogen Sources, Soil Science Society of America Journal, 69(6), 1844, doi:10.2136/sssaj2004.0361, 2005.

Ayers, G. P. and J. L. Gras (1983), The Concentration of Ammonia in Southern-Ocean Air, Journal of Geophysical Research-Oceans and Atmospheres, 88(NC15), 655-659, doi:10.1029/JC088iC15p10655.

Bash, J. O., Walker, J. T., Jones, M., Katul, G., Nemitz, E., and Robarge, W. (2010), Estimation of in-canopy ammonia sources and sinks in a fertilized Zea mays field, Environ. Sci. Technol., 44, 1683– 1689.

Batjes, N.: ISRIC-WISE global data set of derived soil properties on a 0.5 by 0.5 degree grid (Version 3.0), ISRIC-World Soil Inf. Rep, 8, the Netherlands, 24 pp., 2005.

Bernal, M. P. and H. Kirchmann (1992), Carbon and Nitrogen Mineralization and Ammonia Volatilization from Fresh, Aerobically and Anaerobically Treated Pig Manure during Incubation with Soil, Biol. Fertility Soils, 13(3), 135-141.

Beusen, A.H.W., Dekkers, A.L.M., Bouwman, A.F., Ludwig, W. and Harrison, J. (2005) Estimation of global river transport of sediments and associated particulate C, N, and P, Global Biogeochemical Cycles, 19 (2005), p. GB4S05 http://dx.doi.org/10.1029/2005GB002453

Beusen, A. H. W., A. F. Bouwman, P. S. C. Heuberger, G. Van Drecht, and K. W. Van Der Hoek (2008), Bottom-up uncertainty estimates of global ammonia emissions from global agricultural production systems, Atmos. Environ., 42(24), 6067-6077, doi:10.1016/j.atmosenv.2008.03.044.

Black, A. S., R. R. Sherlock, N. P. Smith, K. C. Cameron, and K. M. Goh (1985), Effects of Form of Nitrogen, Season, and Urea Application Rate on Ammonia Volatilization from Pastures, N. Z. J. Agric. Res., 28(4), 469-474.

Black, A., R. Sherlock, N. Smith, and K. Cameron (1989), Ammonia Volatilization from Urea Broadcast in Spring on to Autumn-Sown Wheat, N. Z. J. Crop Hortic. Sci., 17(2), 175-182.

Bodirsky, B. L., Popp, A., Weindl, I., Dietrich, J. P., Rolinski, S., Scheiffele, L., Schmitz, C. and Lotze-Campen, H. (2012), N2O emissions from the global agricultural nitrogen cycle – current state and future scenarios, Biogeosciences, 9(10), 4169–4197, doi:10.5194/bg-9-4169-2012.

Bouwman, A. F., D. S. Lee, W. A. H. Asman, F. J. Dentener, K. W. VanderHoek, and J. G. J. Olivier (1997), A global high-resolution emission inventory for ammonia, Global Biogeochem. Cycles, 11(4), 561-587, doi:10.1029/97GB02266.

Bouwman, L., K. K. Goldewijk, Van Der Hoek, K. W., A. H. W. Beusen, D. P. Van Vuuren, J. Willems, M. C. Rufino, and E. Stehfest (2013), Exploring global changes in nitrogen and phosphorus cycles in agriculture induced by livestock production over the 1900–2050 period, Proceedings of the National Academy of Sciences, doi:10.1073/pnas.1012878108.

Bouwman, A. F., L. J. M. Boumans, and N. H. Batjes (2002), Estimation of global NH3 volatilization loss from synthetic fertilizers and animal manure applied to arable lands and grasslands, Global Biogeochem. Cycles, 16(2), 1024, doi:10.1029/2000GB001389.

Bouwman, L., Goldewijk, K. K., Van Der Hoek, K. W., Beusen, A. H. W., Van Vuuren, D. P., Willems, J., Rufino, M. C. and Stehfest, E. (2013), Exploring global changes in nitrogen and phosphorus cycles in agriculture induced by livestock production over the 1900-2050 period., Proceedings of the National Academy of Sciences of the United States of America, 110(52), 20882–7, doi:10.1073/pnas.1012878108

Bowman, D. C., J. L. Paul, W. B. Davis, and S. H. Nelson (1987), Reducing Ammonia Volatilization from Kentucky Bluegrass Turf by Irrigation, HortScience, 22(1), 84-87.

Branstetter, M. L., and D. J. Erickson, III (2003), Continental runoff dynamics in the Community Climate System Model 2 (CCSM2) control simulation. *J. Geophys. Res., 108(D17), 4550*, doi:10.1029/2002JD003212.

Brouder, S., B. Hofmann, E. Kladivko, R. Turco, A. Bongen, and J. Frankenberger (2005), Interpreting Nitrate Concentration in Tile Drainage Water, Agronomy Guide, Purdue Extension, AY-318-W(1).

Bussink, D. W. (1992), Ammonia Volatilization from Grassland Receiving Nitrogen-Fertilizer and Rotationally Grazed by Dairy-Cattle, Fertilizer Research, 33(3), 257-265, doi:10.1007/BF01050881.

Bussink, D. W. (1994), Relationships between Ammonia Volatilization and Nitrogen-Fertilizer Application Rate, Intake and Excretion of Herbage Nitrogen by Cattle on Grazed Swards, Fertilizer Research, 38(2), 111-121, doi:10.1007/BF00748771.

Canter, L. W. (1996), Nitrates in Groundwater, CRC Press.

Cape, J. N., L. J. van der Eerden, L. J. Sheppard, I. D. Leith, and M. A. Sutton (2009), Reassessment of Critical Levels for Atmospheric Ammonia.

Catchpoole, V., D. Oxenham, and L. Harper (1983), Transformation and Recovery of Urea Applied to a Grass Pasture in Southeastern Queensland, Aust. J. Exp. Agric., 23(120), 80-86, doi:10.1071/EA9830080.

Chae, Y. M. and M. A. Tabatabai (1986), Mineralization of Nitrogen in Soils Amended with Organic Wastes, J. Environ. Qual., 15(2), 193-198.

Chambers, B. J., Lord, E. I., Nicholson, F. A. and Smith, K. A. (1999). Predicting nitrogen availability and losses following application of organic manures to arable land : MANNER. Soil Use and Management, 15, 137-143.

Cooter, E. J., J. O. Bash, J. T. Walker, M. R. Jones, and W. Robarge (2010), Estimation of NH3 bi-directional flux from managed agricultural soils, Atmos. Environ., 44(17), 2107-2115, doi:10.1016/j.atmosenv.2010.02.044.

Dai, A. and K.E. Trenberth (2002), Estimates of freshwater discharge from continents: Latitudinal and seasonal variations, *J. of Hydrometeorology 3*, 660-687.

Davidson, E. A. (2009), The contribution of manure and fertilizer nitrogen to atmospheric nitrous oxide since 1860, Nature Geoscience, 2(9), 659-662, doi:10.1038/NGEO608.

Davidson, E. S. (2012), Representative concentration pathways and mitigation scenarios for nitrous oxide, Environ. Res. Lett., 7, 024005 (7pp), doi:10.1088/1748-9326/7/2/024005.

De Meij, A., Krol, M., Dentener, F., Vignati, E., Cuvelier, C. and Thunis, P. (2006), The sensitivity of aerosol in Europe to two different emission inventories and temporal distribution of emissions, Atmospheric Chemistry and Physics, 6(12), 4287–4309, doi:10.5194/acp-6-4287-2006.

Denmead, O. T., Freney, J. R., and Dunin, F. X. (2008), Gas exchange between plant canopies and the atmosphere: case-studies for ammonia, Atmos. Environ., 42, 3394–3406.

Dentener F.J. and Crutzen P.J. 1994. A three-dimensional model of the global ammonia cycle. J. Atmos. Chem. 19:331-369.

Dumont, E., Harrison,J.A., Kroeze, C., Bakker, E.j. and Seitzinger S.P. (2005) Global distribution and sources of dissolved inorganic nitrogen export to the coastal zone: results from a spatially explicit, global model, Global Biogeochemical Cycles, 19 (2005), p. GB4S02 http://dx.doi.org/10.1029/2005GB002488

EDGAR, 2013: Emissions Database for Global Atmospheric Research (EDGAR). [Available online at http://edgar.jrc.ec.europa.eu].

Eghball, B. and J. E. Gilley (1999), Phosphorus and nitrogen in runoff following beef cattle manure or compost application, J. Environ. Qual., 28(4), 1201-1210.

Eghball, B. (2000), Nitrogen Mineralization from Field-Applied Beef Cattle Feedlot Manure or Compost, Soil Science Society of America Journal, 64, 2024, doi:10.2136/sssaj2000.6462024x.

Eghball, B., B. J. Wienhold, J. E. Gilley, and R. A. Eigenberg (2002), Mineralization of manure nutrients, J. Soil Water Conserv., 57(6), 470-473.

EPA (2010) U.S. Environmental Protection Agency - Managing Agricultural Fertilizer Application to Prevent Contamination of Drinking Water. [Available online at http://www.epa.gov/safewater/sourcewater/pubs/fs_swpp_fertilizer.pdf].

FAO (2005) Food and Agriculture Organization -Data on land use, fertilizer management and environment. [Available online at http://www.fao.org/docrep/004/Y2780E/y2780e05.htm].

Flesch, T. K., J. D. Wilson, L. A. Harper, R. W. Todd, and N. A. Cole (2007), Determining ammonia emissions from a cattle feedlot with an inverse dispersion technique, Agric. For. Meteorol., 144(1-2), 139-155.

Flechard, C. R., Massad, R.-S., Loubet, B., Personne, E., Simpson, D., Bash, J. O., Cooter, E. J., Nemitz, E. and Sutton, M. A. (2013), Advances in understanding, models and parameterizations of biosphere-atmosphere ammonia exchange, Biogeosciences, 10(7), 5183–5225, doi:10.5194/bg-10-5183-2013.

Fowler, D., Coyle, M., Skiba, U., Sutton, M. A., Cape, J. N., Reis, S., Sheppard, L. J., Jenkins, A., Grizzetti, B. and J. N. Galloway (2013) The global nitrogen cycle in the twenty-first century. Philos. Trans. R. Soc. Lond. B. Biol. Sci., 368:20130164

Gale, E. S., D. M. Sullivan, C. G. Cogger, A. I. Bary, D. D. Hemphill, and E. A. Myhre (2006), Estimating plant-available nitrogen release from manures, composts, and specialty products, J. Environ. Qual., 35(6), 2321-2332, doi:10.2134/jeq2006.0062.

Galloway, J. N., F. J. Dentener, D. G. Capone, E. W. Boyer, R. W. Howarth, S. P. Seitzinger, G. P. Asner, C. C. Cleveland, P. A. Green, E. A. Holland, D. M. Karl, A. F. Michaels, J. H. Porter, A. R. Townsend, and C. J. Vorosmarty (2004), Nitrogen cycles: past, present, and future, Biogeochemistry, 70(2), 153-226, doi:10.1007/s10533-004-0370-0.

Génermont, S. and Cellier, P. (1997), A mechanistic model for estimating ammonia volatilization from slurry applied to bare soil, Agricultural and Forest Meteorology, 88(97), 145–167, doi:10.1016/S0168-1923(97)00044-0.

Gilbert, P. M., Harrison, J., Heil, C. and Seitzinger, S. (2006), Escalating Worldwide use of Urea – A Global Change Contributing to Coastal Eutrophication, Biogeochemistry, 77(3), 441–463, doi:10.1007/s10533-005-3070-5.

Gilmour, J. T., Cogger, C. G., Jacobs, L. W., Evanylo, G. K. and Sullivan, D. M. (2003), Decomposition and plant-available nitrogen in biosolids: laboratory studies, field studies, and computer simulation., Journal of environmental quality, 32(4), 1498–507.

Goebes, M. D., R. Strader, and C. Davidson (2003), An ammonia emission inventory for fertilizer application in the United States, Atmos. Environ., 37(18), 2539-2550, doi:10.1016/S1352-2310(03)00129-8.

Grosso, S. J. Del, Parton, W. J., Mosier, A. R., Ojima, D. S., Kulmala, A. E. and Phongpan, S. (2000), General model for N_2O and N_2 gas emissions from soils when comparing observed and gas emission rates from irrigated field soils used for model testing NO2, , 14(4), 1045–1060.

Gu, B., Sutton, M. A., Chang, S. X., Ge, Y. and Chang, J. (2014), Agricultural ammonia emissions contribute to China's urban air pollution, Frontiers in Ecology and the Environment, 12(5), 265–266, doi:10.1890/14.WB.007.

Gusman, A. J. and Mariño, M. A. (1999), Analytical Modeling of Nitrogen Dynamics in Soils and Ground Water, Journal of Irrigation and Drainage Engineering, 125(6), 330–337, doi:10.1061/(ASCE)0733-9437(1999)125:6(330).

Hamaoui-Laguel, L., Meleux, F., Beekmann, M., Bessagnet, B., Génermont, S., Cellier, P. and Létinois, L. (2014), Improving ammonia emissions in air quality modelling for France, Atmospheric Environment, 92, 584–595, doi:10.1016/j.atmosenv.2012.08.002, 2014.

Hargrove, W. L. and D. E. Kissel (1979), Ammonia Volatilization from Surface Applications of Urea in the Field and Laboratory, Soil Sci. Soc. Am. J., 43(2), 359-363.

Harper, L. A., Denmead, O. T., and Sharpe, R. R. (2000), Identifying sources and sinks of scalars in a corn canopy with inverse Lagrangian dispersion analysis II. Ammonia, Agr. Forest Meteorol., 104, 75–83.

Hauglustaine, D. A., Balkanski, Y. and Schulz, M. (2014), A global model simulation of present and future nitrate aerosols and their direct radiative forcing of climate, Atmospheric Chemistry and Physics Discussions, 14(5), 6863–6949, doi:10.5194/acpd-14-6863-2014.

Heald, C. L., Collett, J. L., Lee, T., Benedict, K. B., Schwandner, F. M., Li, Y., Clarisse, L., Hurtmans, D. R., Van Damme, M., Clerbaux, C., Coheur, P. F., Philip, S., Martin, R. V. and Pye, H. O. T.: Atmospheric ammonia and particulate inorganic nitrogen over the United States, Atmospheric Chemistry and Physics, 12, 10295–10312, doi:10.5194/acp-12-10295-2012, 2012.

Holland, E. A., J. Lee-Taylor, C. D. Nevison, and J. Sulzman (2005), Global N Cycle: Fluxes and N2O Mixing Ratios Originating from Human Activity. Data set. Available on-line [http://www.daac.ornl.gov], Oak Ridge National Laboratory Distributed Active Archive Center, Oak Ridge, Tennessee, U.S.A., doi:10.3334/ORNLDAAC/797.

Howarth, R. W., A. Sharpley, and D. Walker (2002), Sources of nutrient pollution to coastal waters in the United States: Implications for achieving coastal water quality goals, Estuaries, 25(4B), 656-676, doi:10.1007/BF02804898.

Huang, X., Y. Song, M. Li, J. Li, Q. Huo, X. Cai, T. Zhu, M. Hu, and H. Zhang (2012), A high-resolution ammonia emission inventory in China, Global Biogeochem. Cycles, 26, GB1030, doi:10.1029/2011GB004161.

Hudman, R. C., Russell, a. R., Valin, L. C. and Cohen, R. C. (2010), Interannual variability in soil nitric oxide emissions over the United States as viewed from space, Atmospheric Chemistry and Physics, 10(20), 9943–9952, doi:10.5194/acp-10-9943-2010.

Hurrell, J. W., et al. (2013), The Community Earth System Model: A Framework for Collaborative Research, *Bulletin of the American Meteorological Society*, 0.1175/BAMS-D-1112-00121.

Jackson, R. D., W. P. Kustas, and B. J. Choudhury (1988), A Reexamination of the Crop Water-Stress Index, Irrig. Sci., 9(4), 309-317, doi:10.1007/BF00296705.

Jarvis, S. C., D. J. Hatch, and D. R. Lockyer (1989), Ammonia Fluxes from Grazed Grassland - Annual Losses from Cattle Production Systems and their Relation to Nitrogen Inputs, J. Agric. Sci., 113, 99-108.

Jury, W. A., Spencer, W. F. and Farmer, W. J. (1983), Behavior Assessment Model for Trace Organics in Soil: I. Model Description1, Journal of Environment Quality, 12(4), 558, doi:10.2134/jeq1983.00472425001200040025x.

Keppel-Aleks, G., and Coauthors, 2013: Evolution of atmospheric carbon dioxide variabilty during the 21st century in a coupled carbon-climate model. Journal of Climate, 26, doi:10.1175/JCLI-D1112-00589.00581.

King, K. W. and J. C. Balogh (2000), Development of a nitrogen-release algorithm for slow-release fertilizers, Trans. ASAE, 43(3), 661-664.

Koven, C. D., Riley, W. J., Subin, Z. M., Tang, J. Y., Torn, M. S., Collins, W. D., Bonan, G. B., Lawrence, D. M. and Swenson, S. C. (2013), The effect of vertically resolved soil biogeochemistry and alternate soil C and N models on C dynamics of CLM4, Biogeosciences, 10(11), 7109–7131, doi:10.5194/bg-10-7109-2013.

Lamarque, J.-F., Bond, T., Eyring, V., Granier, C., Heil, A., Klimont, Z., Lee, D., Liousse, C., Mieville, A., Owen, B., Schulz, M., Schindell, D., Smith, S., Stehfest, E., VanAardenne, J., Cooper, O., Kainuma, M., Mahowald, N., McConnell, J., Naik, V., Riahi, K., Van Vuurent, D., 2010. Historical (1850-200) gridded anthropogenic and biomass burning emissions of reactive gases and aerosols: methodology and application. Atmospheric Chemistry and Physics 10, 7017-7039.

Lamarque, J.-F., Shindell, D. T., Josse, B., Young, P. J., Cionni, I., Eyring, V., Bergmann, D., Cameron-Smith, P., Collins, W. J., Doherty, R., Dalsoren, S., Faluvegi, G., Folberth, G., Ghan, S. J., Horowitz, L. W., Lee, Y. H., MacKenzie, I. A., Nagashima, T., Naik, V., Plummer, D., Righi, M., Rumbold, S. T., Schulz, M., Skeie, R. B., Stevenson, D. S., Strode, S., Sudo, K., Szopa, S., Voulgarakis, A. and Zeng, G. (2013), The Atmospheric Chemistry and Climate Model Intercomparison Project (ACCMIP): overview and description of models, simulations and climate diagnostics, Geoscientific Model Development, 6(1), 179–206, doi:10.5194/gmd-6-179-2013.

Lawrence, D. M., P. E. Thornton, K. W. Oleson, and G. B. Bonan (2007), The partitioning of evapotranspiration into transpiration, soil evaporation, and canopy evaporation in a GCM: Impacts on land-atmosphere interaction, J. Hydrometeorol., 8(4), 862-880, doi:10.1175/JHM596.1.

Lawrence, D. M., K.W. Oleson, M.G. Flanner, C.G. Fletcher, P.J. Lawrence, S. S. Levis, C. Swenson, and G.B. Bonan (2012), The CCSM4 land simulation, 1850-2005: Assessment of surface climate and new capabilities, *J. Climate*, *25*(7), 2240-2260.

Lindsay, K., G. Bonan, S. Doney, F. Hofffman, D. Lawrence, M. C. Long, N. Mahowald, J. K. Moore, J. T. Randerson, and P. Thornton (2014), Preindustrial and 20th century experiments with the Earth System Model CESM1-(BGC), *Journal of Climate*, *27*, 8981-9005.

Levis, S., G. B. Bonan, E. Kluzek, P. E. Thornton, A. Jones, W. J. Sacks, and C. J. Kucharik, (2012),Interactive Crop Management in the Community Earth System Model (CESM1): Seasonal Influences on Land–Atmosphere Fluxes. *J. Climate*, **25**, 4839–4859.doi: http://dx.doi.org/10.1175/JCLI-D-11-00446.1

Li, C., Salas, W., Zhang, R., Krauter, C., Rotz, A. and Mitloehner, F. (2012), Manure-DNDC: a biogeochemical process model for quantifying greenhouse gas and ammonia emissions from livestock manure systems, Nutrient Cycling in Agroecosystems, 93(2), 163–200, doi:10.1007/s10705-012-9507-z.

Lindsay, K., and Coauthors, in press: Preindustrial and 20th century experiments with the Earth System Model CESM1-(BGC). Journal of Climate.

Loubet, B., W. A. H. Asman, M. R. Theobald, O. Hertel, Y. S. Tang, P. Robin, M. Hassouna, U. Daemmgen, S. Genermont, P. Cellier, and M. A. Sutton (2009), Ammonia Deposition Near Hot Spots: Processes, Models and Monitoring Methods.

Massad, R. S., Nemitz, E., and. Sutton, M. A. (2010) Review and parameterization of bi-directional ammonia exchange between vegetation and the atmosphere, Atmos. Chem. Phys., 10, 10359–10386,doi:10.5194/acp-10-10359-2010.

Mayorga, E., Seitzinger, S. P., Harrison, J. A., Dumont, E., Beusen, A. H. W., Bouwman, A. F., Fekete, B. M., Kroeze, C. and Van Drecht, G. (2010), Global Nutrient Export from WaterSheds 2 (NEWS 2): Model development and implementation, Environmental Modelling & Software, 25(7), 837–853, doi:10.1016/j.envsoft.2010.01.007.

Meyer, R. L., T. Kjaer, and N. P. Revsbech (2002), Nitrification and denitrification near a soil-manure interface studied with a nitrate-nitrite biosensor, Soil Sci. Soc. Am. J., 66(2), 498-506.

Mitsch, W., J. and J. G. Gosselink (2007), Wetlands, John Wiley and Sons, Hoboken, NJ.

Motavalli, P. P., K. A. Kelling, and J. C. Converse (1989), 1st-Year Nutrient Availability from Injected Dairy Manure, J. Environ. Qual., 18(2), 180-185.

Mulvaney, M. J., K. A. Cummins, C. W. Wood, B. H. Wood, and P. J. Tyler (2008), Ammonia Emissions from Field-Simulated Cattle Defecation and Urination, J. Environ. Qual., 37(6), 2022-2027, doi:10.2134/jeq2008.0016.

Myhre, G., Samset, B. H., Schulz, M., Balkanski, Y., Bauer, S., Berntsen, T. K., Bian, H., Bellouin, N., Chin, M., Diehl, T., Easter, R. C., Feichter, J., Ghan, S. J., Hauglustaine, D., Iversen, T., Kinne, S., Kirkevåg, A., Lamarque, J.-F., Lin, G., Liu, X., Lund, M. T., Luo, G., Ma, X., van Noije, T., Penner, J. E., Rasch, P. J., Ruiz, A., Seland, Ø., Skeie, R. B., Stier, P., Takemura, T., Tsigaridis, K., Wang, P., Wang, Z., Xu, L., Yu, H., Yu, F., Yoon, J.-H., Zhang, K., Zhang, H. and Zhou, C. (2013), Radiative forcing of the direct aerosol effect from AeroCom Phase II simulations, Atmospheric Chemistry and Physics, 13(4), 1853–1877, doi:10.5194/acp-13-1853-2013.

Nason, G. E. and D. D. Myrold (1992), Nitrogen fertilizers: fates and environmental effects in forests, in Forest fertilization: Sustaining and improving nutrition and growth of western forests, edited by H. N. Chappell et al, pp. 67-81.

Nemitz, E., C. Milford, and M. A. Sutton (2001), A two-layer canopy compensation point model for describing bi-directional biosphere-atmosphere exchange of ammonia, Q. J. R. Meteorol. Soc., 127(573), 815-833, doi:10.1256/smsqj.57305.

Nemitz, E., M. A. Sutton, J. K. Schjoerring, S. Husted, and G. P. Wyers (2000), Resistance modelling of ammonia exchange over oilseed rape, Agric. For. Meteorol., 105(4), 405-425, doi:10.1016/S0168-1923(00)00206-9.

Nevison, C. D., P.G. Hess, S. Riddick and D. Ward (2016), Denitrification, leaching and river nitrogen export in the Community Land Model, *J. Adv. Model. Earth Syst.,8*, doi: 10.1002/2015MS000573, 2016.

Oleson, K. W., G. -. Niu, Z. -. Yang, D. M. Lawrence, P. E. Thornton, P. J. Lawrence, R. Stoeckli, R. E. Dickinson, G. B. Bonan, S. Levis, A. Dai, and T. Qian (2008), Improvements to the Community Land Model and their impact on the hydrological cycle, Journal of Geophysical Research-Biogeosciences, 113(G1), G01021, doi:10.1029/2007JG000563.

Parton, W. J., D. S. Schimel, C. V. Cole, and D. S. Ojima (1987), Analysis of Factors Controlling Soil Organic-Matter Levels in Great-Plains Grasslands, Soil Sci. Soc. Am. J., 51(5), 1173-1179.

Parton, W. J., Mosier, A. R., Ojima, D. S., Valentine, D. W., Schimel, D. S., Weier, K. and Kulmala, A. E. (1996), Generalized model for N2 and N2O production from nitrification and denitrification, GLOBAL BIOGEOCHEMICAL CYCLES, 10(3), 401–412.

Parton, W. J., Holland, E. A., Grosso, S. J. Del, Hartman, M. D., Martin, R. E., Mosier, A. R., Ojima, D. S. and Schimel, D. S. (2001), Generalized model for NOx and NzO emissions from soils, J. Geophys. Res, 106, 17,403–17,491.

Pinder, R. W., Pekney, N. J., Davidson, C. I. and Adams, P. J. (2004), A process-based model of ammonia emissions from dairy cows: Improved temporal and spatial resolution, Atmospheric Environment, 38, 1357–1365, doi:10.1016/j.atmosenv.2003.11.024.

Pinder, R. W., J. T. Walker, J. O. Bash, K. E. Cady-Pereira, D. K. Henze, M. Luo, G. B. Osterman, and M. W. Shephard (2011), Quantifying spatial and temporal variability in atmospheric ammonia with in situ and space-based observations, Geophys. Res. Lett., 38, L04802, *doi:*10.1029/2010GL046146.

Potter, P., N. Ramankutty, E. M. Bennett, and S. D. Donner (2010), Characterizing the Spatial Patterns of Global Fertilizer Application and Manure Production, Earth Interact., 14, 2, doi:10.1175/2009EI288.1.

Paulot, F., D. J. Jacob, R. W. Pinder, J. O. Bash, K. Travis, and D. K. Henze (2014), Ammonia emissions in the United States, European Union, and China derived by high-resolution inversion of ammonium wet deposition data: Interpretation with a new agricultural emissions inventory (MASAGE_NH3), J. Geophys. Res. Atmos., 119, 4343–4364, doi:10.1002/2013JD021130.

Qian, T., Dai, A., Trenberth, K. E. and Oleson, K. W. (2006), Simulation of Global Land Surface Conditions from 1948 to 2004. Part I: Forcing Data and Evaluations, Journal of Hydrometeorology, 7(5), 953–975, doi:10.1175/JHM540.1.

Randerson, J. T., F. M. Hoffman, P. E. Thornton, N. M. Mahowald, K. Lindsay, Y. Lee, C. D. Nevison, S. C. Doney, G. Bonan, R. Stoeckli, C. Covey, S. W. Running, and I. Y. Fung (2009), Systematic assessment of terrestrial biogeochemistry in coupled climate-carbon models, Global Change Biol., 15(10), 2462-2484, doi:10.1111/j.1365-2486.2009.01912.x.

Riddick (2012) The global ammonia emission from seabirds. PhD thesis, King's College, London.

Riddick, S. N., U. Dragosits, T. D. Blackall, F. Daunt, S. Wanless, and M. A. Sutton (2012), The global distribution of ammonia emissions from seabird colonies, Atmos. Environ., 55, 319-327, doi:10.1016/j.atmosenv.2012.02.052.

Sanz, A., Misselbrook, T., Sanz, M. J., and Vallejo, A.: Use of an inverse dispersion technique for estimating ammonia emission from surface-applied slurry, Atmos. Environ., 44, 999–1002, doi:10.1016/j.atmosenv.2009.08.044, 2010.

Shindell, D. T., Lamarque, J.-F., Schulz, M., Flanner, M., Jiao, C., Chin, M., Young, P. J., Lee, Y. H., Rotstayn, L., Mahowald, N., Milly, G., Faluvegi, G., Balkanski, Y., Collins, W. J., Conley, A. J., Dalsoren, S., Easter, R., Ghan, S., Horowitz, L., Liu, X., Myhre, G., Nagashima, T., Naik, V., Rumbold, S. T., Skeie, R., Sudo, K., Szopa, S., Takemura, T., Voulgarakis, A., Yoon, J.-H. and Lo, F. (2013), Radiative forcing in the ACCMIP historical and future climate simulations, Atmospheric Chemistry and Physics, 13(6), 2939–2974, doi:10.5194/acp-13-2939-2013.

Seinfeld, J. H. and S. N. Pandis (2006), Atmospheric Chemistry and Physics: From Air Pollution to Climate Change, John Wiley & Sons, London.

Seitzinger, S.P., Harrison, J.A., Dumont,E., Beusen, A.H. and Bouwman, A.F. (2005) Sources and delivery of carbon, nitrogen, and phosphorus to the coastal zone: an overview of Global Nutrient Export from Watersheds (NEWS) models and their application, Global Biogeochemical Cycles, 19 (2005), p. GB4S01 http://dx.doi.org/10.1029/2005GB002606

Sheard, R. W. and E. G. Beauchamp (1985), Aerodyanmic measurement of ammonium volatilization from urea applied to bluegrass fescue turf, paper presented at 5th Int. Turfgrass Res. Conf., Avignon, France. 1-5 July. INRA Paris, France.

Sintermann, J., Ammann, C., Kuhn, U., Spirig, C., Hirschberger, R., Gärtner, A., and Neftel, A.: Determination of field scaleammonia emissions for common slurry spreading practice with two independent methods, Atmos. Meas. Tech., 4, 1821–1840, doi:10.5194/amt-4-1821-2011, 2011.

Skjøth, C. A., Geels, C., Berge, H., Gyldenkærne, S., Fagerli, H., Ellermann, T., Frohn, L. M., Christensen, J., Hansen, K. M., Hansen, K. and Hertel, O. (2011): Spatial and temporal variations in ammonia emissions – a freely accessible model code for Europe, Atmospheric Chemistry and Physics, 11(11), 5221–5236, doi:10.5194/acp-11-5221-2011.

Skjøth, C. A. and C. Geels (2013), The effect of climate and climate change on ammonia emissions in Europe, Atmospheric Chemistry and Physics, 13(1), 117-128, doi:10.5194/acp-13-117-2013.

Smil, V. (2000), Feeding the world: a challenge for the twenty-first century. Cambridge, MA, USA: MIT Press, 388 pp

Smith, L.W. (1973) Nutritive evaluations of animal manures. Symposium: processing agricultural and municipal wastes. George E. Inglett (Ed.). Avi. Publ. Co., Westport, CT.

Sommer, S. G., Hutchings, N.J. (2001), Ammonia emission from field applied manure and its reduction—invited paper, European Journal of Agronomy, 15, 1 – 15.

Sparks, J. P. (2009), Ecological ramifications of the direct foliar uptake of nitrogen., Oecologia, 159(1), 1–13, doi:10.1007/s00442-008-1188-6.

Spirig, C., Flechard, C. R., Ammann, C., and Neftel, A.: The annual ammonia budget of fertilised cut grassland – Part 1: Micrometeorological flux measurements and emissions after slurry applica- tion, Biogeosciences, 7, 521–536, doi:10.5194/bg-7-521-2010, 2010.

Stange, C. F. and H. -. Neue (2009), Measuring and modelling seasonal variation of gross nitrification rates in response to long-term fertilisation, Biogeosciences, 6(10), 2181-2192.

Steenvoorden, J. H. (1989), Nitrogen Cycling in Manure and Soils: Crop Utilization and Environmrntal Losses, paper presented at Dairy Manure Management, Proceedings from the Dairy Manure Management Symposium, Syracuse, NY , 2122-241198.

Stoeckli, R., D. M. Lawrence, G. -. Niu, K. W. Oleson, P. E. Thornton, Z. -. Yang, G. B. Bonan, A. S. Denning, and S. W. Running (2008), Use of FLUXNET in the community land model development, Journal of Geophysical Research-Biogeosciences, 113(G1), G01025, doi:10.1029/2007JG000562.

Sutton, M. A., W. A. H. Asman, and J. K. Schjorring (1994), Dry Deposition of Reduced Nitrogen, Tellus Series B-Chemical and Physical Meteorology, 46(4), 255-273, doi:10.1034/j.1600-0889.1994.t01-2-00002.x.

Sutton, M. A., C. J. Place, M. Eager, D. Fowler, and R. I. Smith (1995), Assessment of the Magnitude of Ammonia Emissions in the United-Kingdom, Atmos. Environ., 29(12), 1393-1411, doi:10.1016/1352-2310(95)00035-W.

Sutton, M. A., S. Reis, G. Billen, P. Cellier, J. W. Erisman, A. R. Mosier, E. Nemitz, J. Sprent, H. van Grinsven, M. Voss, C. Beier, and U. Skiba (2012), "Nitrogen & Global Change" Preface, Biogeosciences, 9(5), 1691-1693, doi:10.5194/bg-9-1691-2012.

Sutton, M. A., S. Reis, S. N. Riddick, U. Dragosits, E. Nemitz, M. R. Theobald, Y. S. Tang, C. F. Braban, M. Vieno, A. J. Dore, R. F. Mitchell, S. Wanless, F. Daunt, D. Fowler, T. D. Blackall, C. Milford, C. R. Flechard, B. Loubet, R. Massad, P. Cellier, E. Personne, P. F. Coheur, L. Clarisse, M. Van Damme, Y. Ngadi, C. Clerbaux, C. A. Skjoth, C. Geels, O. Hertel, R. J. W. Kruit, R. W. Pinder, J. O. Bash, J. T. Walker, D. Simpson, L. Horvath, T. H. Misselbrook, A. Bleeker, F. Dentener, and W. de Vries (2013), Towards a climate-dependent paradigm of ammonia emission and deposition, Philosophical Transactions of the Royal Society B-Biological Sciences, 368(1621), 20130166, doi:10.1098/rstb.2013.0166.

Thomas, R. Q., Bonan, G. B. and Goodale, C. L. (2013), Insights into mechanisms governing forest carbon response to nitrogen deposition: a model–data comparison using observed responses to nitrogen addition, Biogeosciences, 10(6), 3869–3887, doi:10.5194/bg-10-3869-2013.

Thornton, P., J. F. Lamarque, N. A. Rosenbloom, and N. Mahowald, 2007: Influence of carbon-nitrogen cycle coupling on land model response to CO2 fertilization and climate variability. Global Biogeochemical Cycles, 21, doi:10.1029/2006GB002868.

Thornton, P., and Coauthors, 2009: Carbon-nitrogen interactions regular climate-carbon cycle feedbacks: results from an atmosphere-ocean general circulation model. Biogeosciences-discussion, 6, 3303-3354.

Tilman, D., J. Fargione, B. Wolff, C. D'Antonio, A. Dobson, R. Howarth, D. Schindler, W. H. Schlesinger, D. Simberloff, and D. Swackhamer (2001), Forecasting agriculturally driven global environmental change, Science, 292(5515), 281-284, doi:10.1126/science.1057544.

Todd, R.W., Cole, N.A., Harper, L.A., Flesch, T.K. (2007), Flux gradient estimates of ammonia emissions from beef cattle feedyard pens, International Symposium on Air Quality and Waste Management for Agriculture, 16-19 September 2007, Broomfield, Colorado 701P0907cd., doi:10.13031/2013.23877.

Turner, R. E. and N. N. Rabalais (1991), Changes in Mississippi River Water-Quality this Century, Bioscience, 41(3), 140-147, doi:10.2307/1311453.

United Nations Industrial Development Organization (UNIDO) and International Fertilizer Development Center (IFDC) (Eds.) (1988), Fertilizer Manual, Kluwer Academic Publishers, Dordrecht, The Netherland.

USEPA, 2010: United States Environmental Protection Agency, Source Water Protection Practices Bulletin - Managing Agricultural Fertilizer Application to Prevent Contamination of Drinking Water.

Vaio, N., M. L. Cabrera, D. E. Kissel, J. A. Rema, J. F. Newsome, and Calvert,Vaughn H.,,II (2008), Ammonia Volatilization from Urea-Based Fertilizers Applied to Tall Fescue Pastures in Georgia, USA, Soil Sci. Soc. Am. J., 72(6), 1665-1671, doi:10.2136/sssaj2007.0300.

Van Drecht, G., A. F. Bouwman, J. M. Knoop, A. H. W. Beusen, and C. R. Meinardi (2003), Global modeling of the fate of nitrogen from point and nonpoint sources in soils, groundwater, and surface water, Global Biogeochem. Cycles, 17(4), 1115, doi:10.1029/2003GB002060.

Vigil, M. F. and Kissel, D. E.: (1995), Rate of Nitrogen Mineralized from Incorporated Crop Residues as Influenced by Temperature, Soil Science Society of America Journal, 59(6), 1636, doi:10.2136/sssaj1995.03615995005900060019x.

Visek, W. J. (1984) Ammonia: its effects on biological systems, metabolic hormones, and reproduction. Journal Dairy Science, 67, 481-498.

Vitousek P. M., Menge D. N. L., Reed S. C., Cleveland C. C. (2013) Biological nitrogen fixation: rates, patterns and ecological controls in terrestrial ecosystems. Phil Trans R Soc B 368: 20130119. http://dx.doi.org/10.1098/rstb.2013.0119

Vogt, E., C. F. Braban, U. Dragosits, M. R. Theobald, M. F. Billett, A. J. Dore, Y. S. Tang, N. van Dijk, R. M. Rees, C. McDonald, S. Murray, U. M. Skiba, and M. A. Sutton (2013), Estimation of nitrogen budgets for contrasting catchments at the landscape scale, Biogeosciences, 10(1), 119-133, doi:10.5194/bg-10-119-2013

Walker, J.T., W.P. Robarge, Y. Wu, and T.P. Meyers (2006), Measurement of Bi-Directional Ammonia Fluxes over Soybean Using the Modified Bowen-Ratio Technique. *Agricultural and Forest Meteorology* 138, no. 1/4 (2006). ://20063157463.

Wichink Kruit R.J., Schaap M., Sauter F.J., Van Zanten M.C., van Pul W.A.J. (2012) modeling the distribution of ammonia across Europe including bi-directional surface-atmosphere exchange. Biogeosciences 9 , 5261–5277. (doi:10.5194/bg-9-5261-2012)

Wilson, L. J., Bacon, P. J., Bull, J., Dragosits, U., Blackall, T. D., Dunn, T. E., Hamer, K. C., Sutton, M. A., and Wanless, S. (2004), Modelling the spatial distribution of ammonia emissions from seabirds, Environ. Pollut., 131, 173–185.

Whitehead, D. C. and N. Raistrick (1990), Ammonia volatilization from five nitrogen compounds used as fertilizers following surface application to soils, Journal of Soil Science, 41 (3) p. 387-394.

Zbieranowski, A. L. and J. Aherne (2012), Spatial and temporal concentration of ambient atmospheric ammonia in southern Ontario, Canada, Atmos. Environ., 62, 441-450, doi:10.1016/j.atmosenv.2012.08.041.

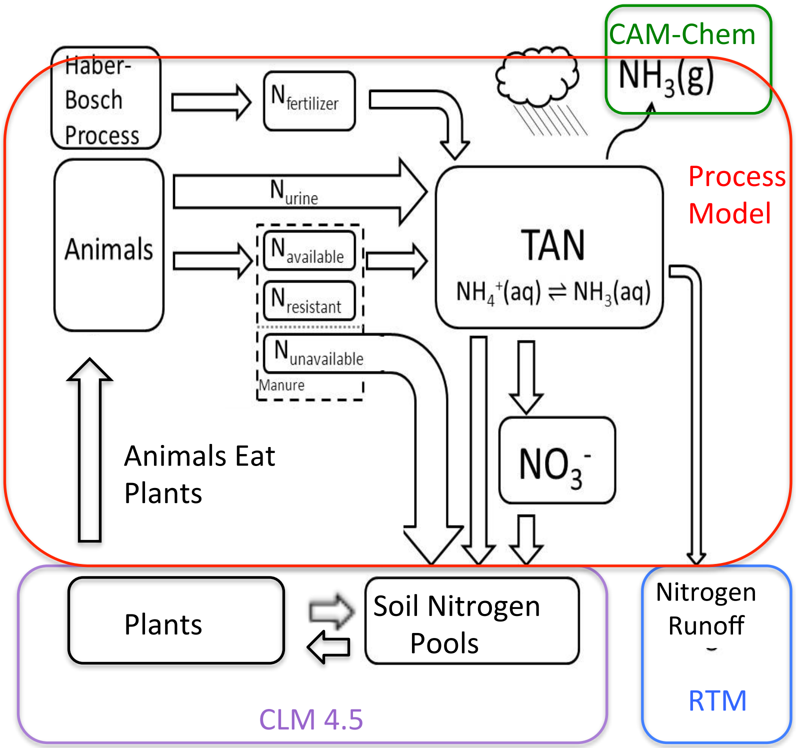

Figure 1. Schematic of the addition of manure and fertilizer (Process Model) to the CESM nitrogen cycle. Some minor pathways are not shown. Soil nitrogen pools and and plant nitrogen exist in CLM4.5. Urine nitrogen (N_{urine}) is directly input to the TAN pool while fecal matter is split into three parts that decompose into the TAN pool at a rate determined by their C: N ratio ($N_{available}$, $N_{resistant}$, $N_{unavailable}$). Manure nitrogen that does not mineralize ($N_{unavailable}$) is added to the soil organic nitrogen pool. Nitrogen applied as synthetic fertilizer is added to the $N_{fertilizer}$ pool where it decomposes into the TAN pool. Losses from the TAN pool include ammonia (NH_3) emission (into CAM-chem), nitrogen run-off (into the RTM), above ground nitrate (NO_3^-) formation and diffusion to the soil nitrogen pools.

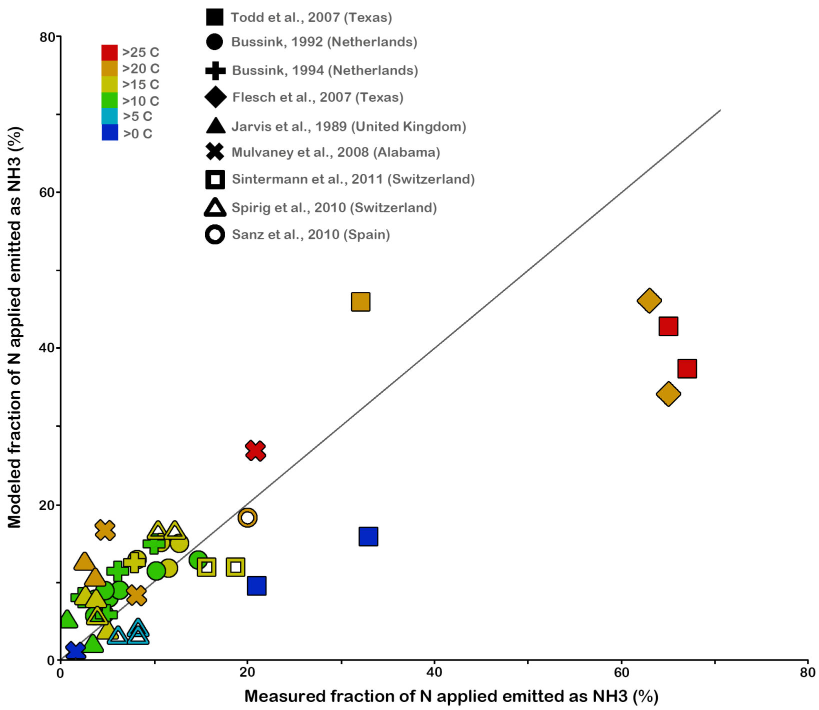

Figure 2. Comparison of model to measurements for percentage of nitrogen lost as NH_3 emissions from manure for a range of studies (see supplementary Table 1). Symbol color measures temperature at which emissions were made; shape gives the study.

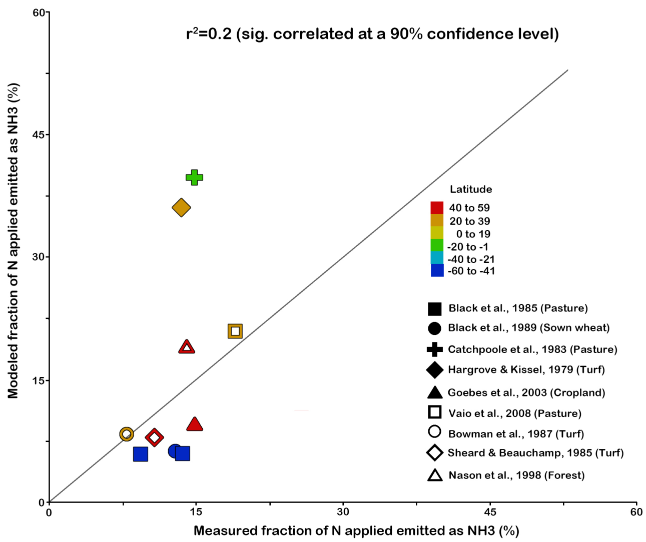

Figure 3. Comparison of model to measurements for percentage of nitrogen lost as NH_3 emissions from fertilizer (see supplementary Table 2). Symbol color gives the latitude at which the measurement was made; symbol shape gives the study and type of fertilizer application.

.

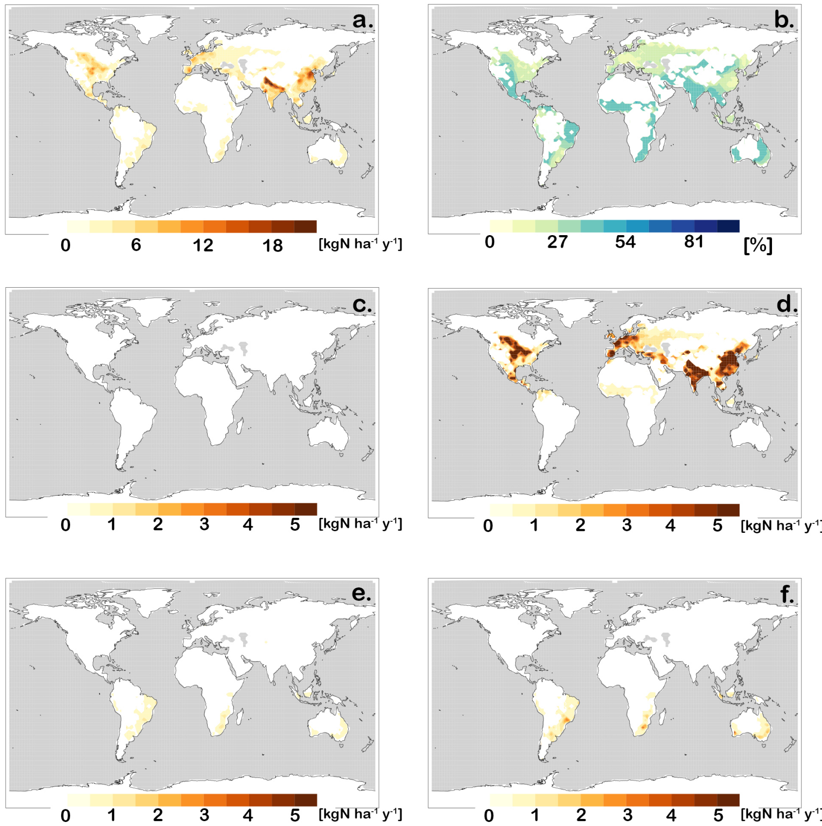

Figure 4. Simulated NH_3 emissions from fertilizer application from 1995-2004 for the present-day control simulation. Simulated emissions (kg N ha^{-1} yr^{-1}) as a) an annual average, c) Jan-Feb-Mar average, d) Apr-May-Jun average, e) Jul-Aug-Sep average, and f) Oct-Nov-Dec average. Simulated emissions as a percent of annual fertilizer application, b).

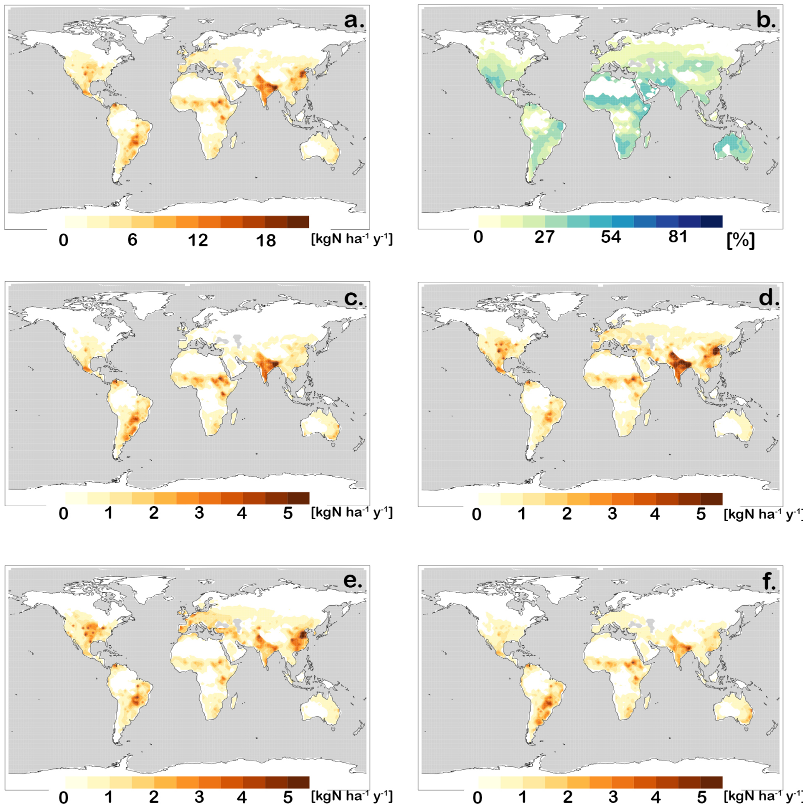

Figure 5. As in Figure 4 but for manure application.

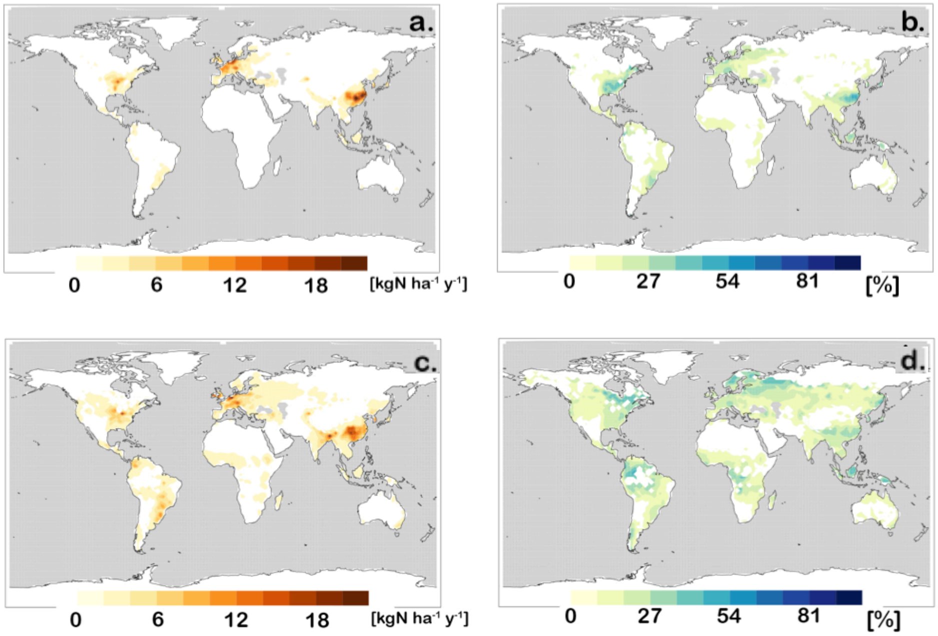

Figure 6. Simulated runoff of N_r from fertilizer and manure TAN pools for the present-day (1995-2004) control simulation. Simulated runoff (kg N ha^{-1} yr^{-1}) as an annual average for a) fertilizer, c) manure. Simulated as a) percent of annual fertilizer application, d) percent of annual manure application.

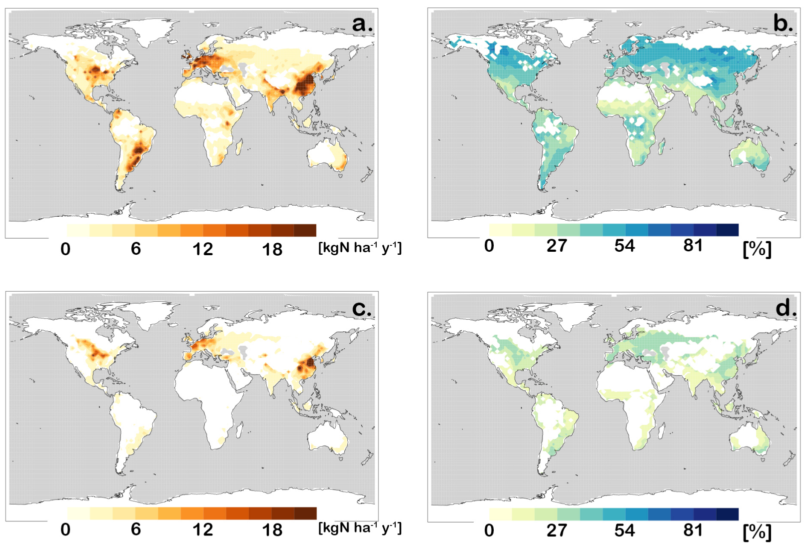

Figure 7. As in Figure 6, but for simulated nitrification.

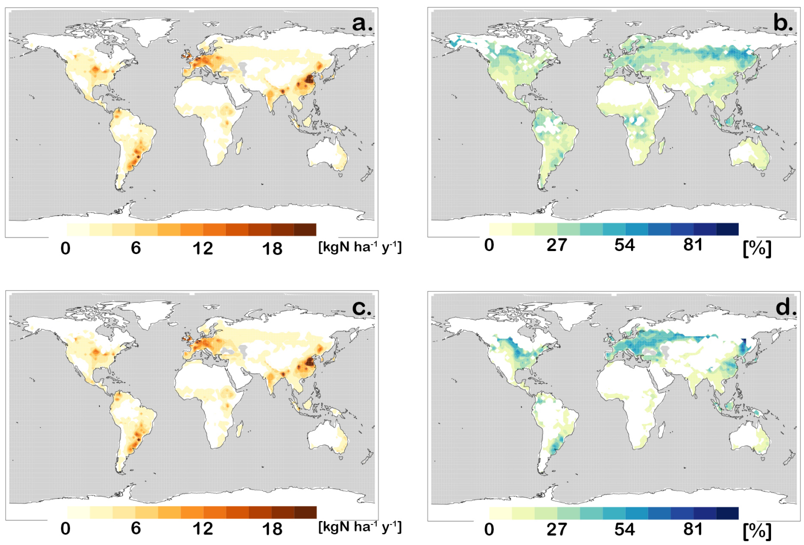

Figure 8. As in Figure 6 but for flux of TAN nitrogen to the soil.

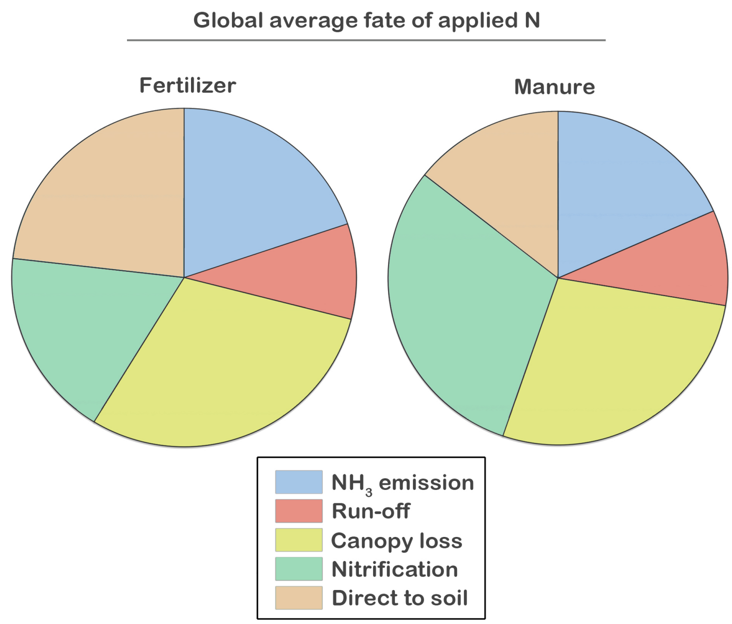

Figure 9. Global Fate of TAN Nr applied as fertilizer (a) or as manure (b). Emissions are split between those to the atmosphere and those captured by the canopy.

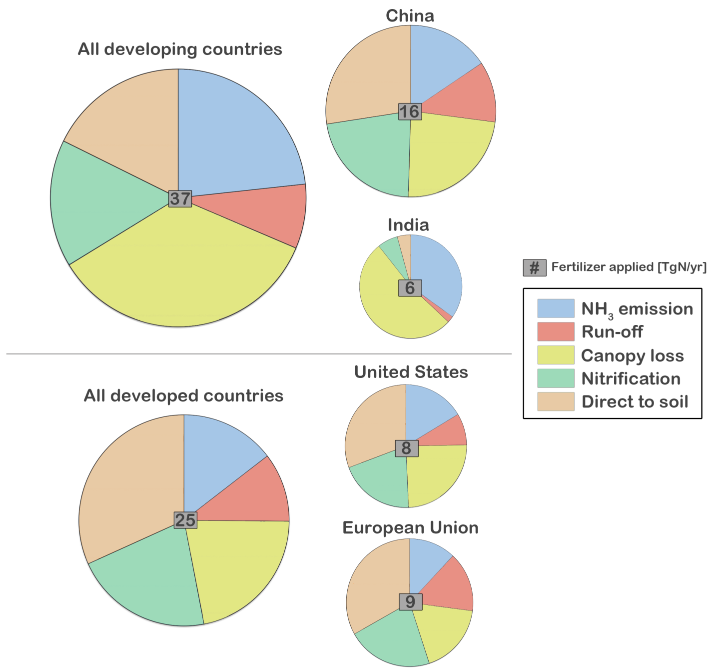

Figure 10. As in Figure 9, but fate of TAN nitrogen by country and region. Countries are split between developed countries and developing countries.

.

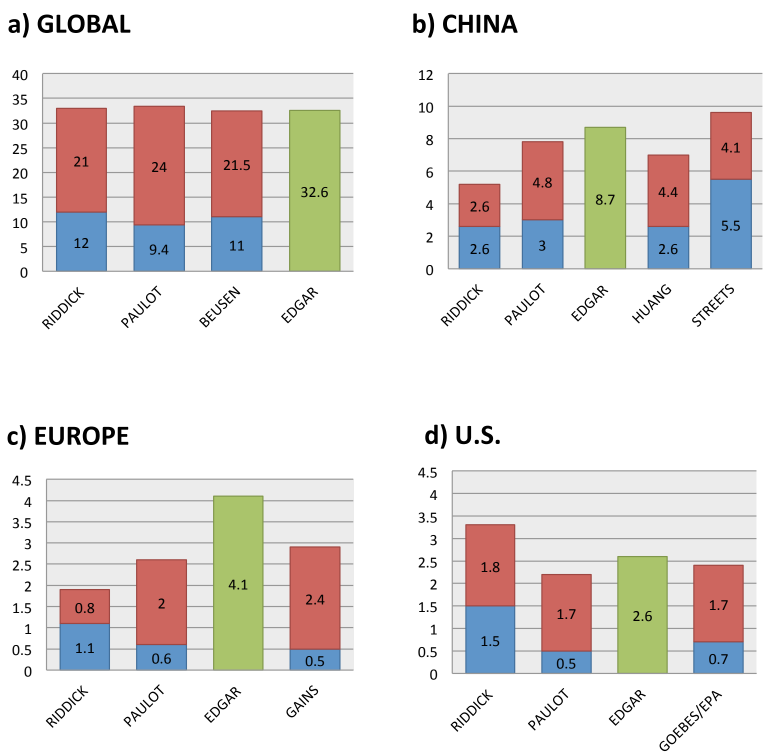

Figure 11. Comparison of manure (red) and synthetic fertilizer (blue) ammonia emissions or combined manure and synthetic fertilzer emissions (green) (Tg N yr^{-1}) a**)** globally, b) China, c) Europe and d) US for this study (Riddick) and for other studies. See text for details.

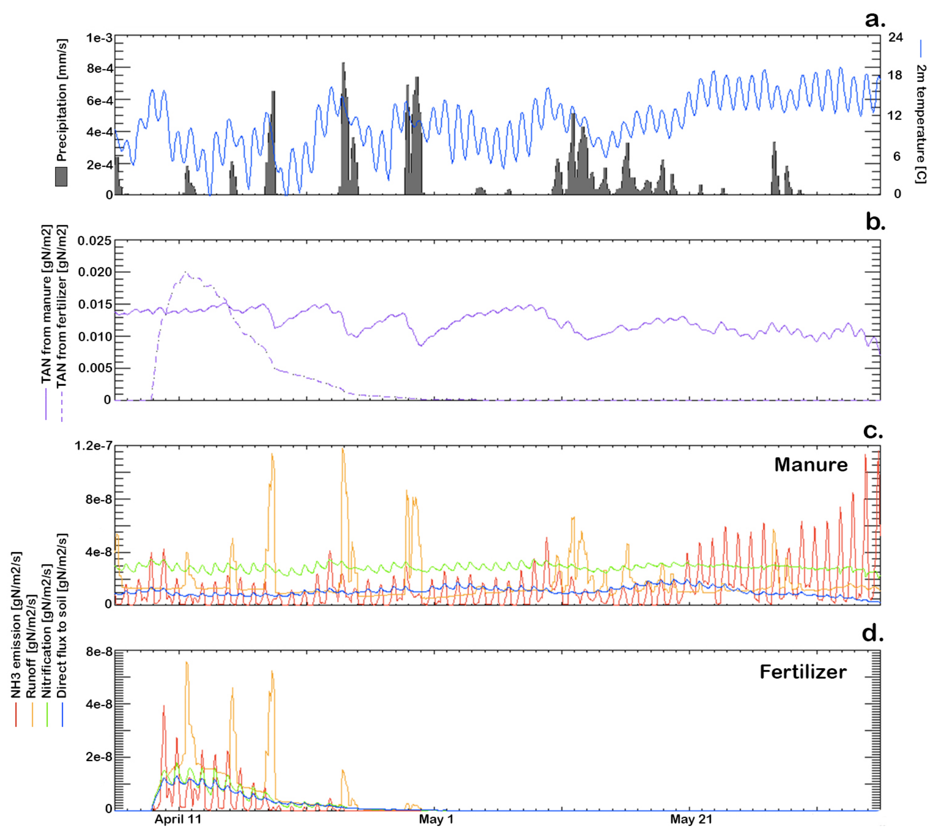

Figure 12. Site specific pathways for nitrogen budget at 35˚N and 100˚W, near the Texas panhandle . Panels show a) the temperature (^{o}C) and precipitation (mm s^{-1}) used to force the CLM, b) the manure (solid) and fertilizer TAN pools (dashed) (gN m^{-2}), and the four major loss pathways from the TAN pools (NH_3 emissions, red; runoff, orange; nitrification, green; diffusion to the soil, blue) (g N m^2 s^{-1}) from c) the manure TAN pool d) the fertilizer TAN pool.

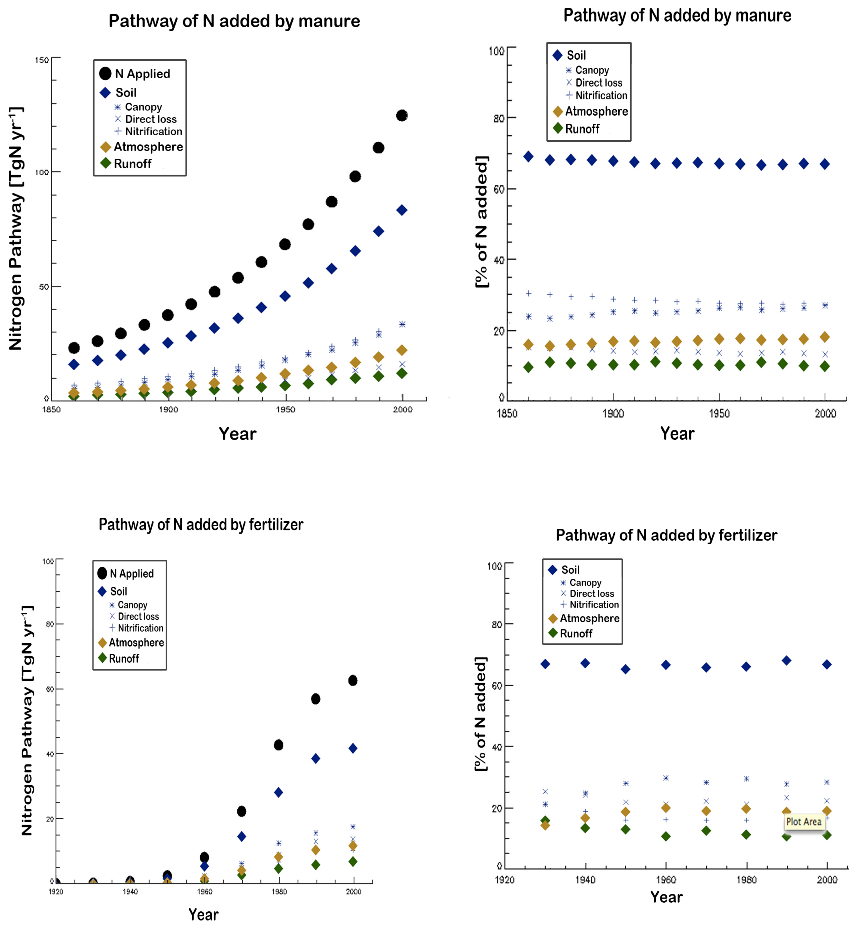

Figure 13. Applied nitrogen and nitrogen losses for the historical simulation in Tg N yr^{-1} for a) manure and c) fertilizer. Nitrogen losses from the TAN pool as a percentage of applied nitrogen for the historical simulation for b) manure and d) fertilizer. The losses from the TAN pool are divided into emission losses of ammonia to the atmosphere (golden diamond), runoff (green diamond) and loss to the soil. Loss to the soil is divided into that due to canopy loss (askerisk) , direct diffusive loss (cross) and nitrification (plus) (see section 3.2.3).